Chongchong Tang, Michael Stueber, Hans Juergen Seifert and Martin Steinbrueck*

Protective coatings on zirconium-based alloys as accident-tolerant fuel (ATF) claddings

DOI 10.1515/corrrev-2017-0010
Received January 25, 2017; accepted May 11, 2017

Abstract: Surface-modified zirconium (Zr)-based alloys, mainly by fabricating protective coatings, are being developed and evaluated as accident-tolerant fuel (ATF) claddings, aiming to improve fuel reliability and safety during normal operations, anticipated operational occurrences, and accident scenarios in water-cooled reactors. In this overview, the performance of Zr alloy claddings under normal and accident conditions is first briefly summarized. In evaluating previous studies, various coating concepts are highlighted based on coating materials, focusing on their performance in autoclave hydrothermal corrosion tests and high-temperature steam oxidation tests. The challenges for the utilization of coatings, including materials selection, deposition technology, and stability under various situations, are discussed to provide some valuable guidance to future research activities.

Keywords: ATF; corrosion; oxidation; protective coatings; Zr-based alloy claddings.

1 Introduction

The continuous growth in electricity demand worldwide with the need of managing atmospheric greenhouse gas emissions simultaneously drives a growing demand for environmentally sustainable electricity generation (Chu & Majumdar, 2012). Nuclear power generation provides a reliable and economic supply of electricity, with very low carbon emissions and relatively small amounts of waste that can be safely stored and eventually disposed (Rogers, 2009). Nuclear power currently provides ~13% of the world's electricity, with more than 400 reactors in operation around the world at the end of 2014 (International Atomic Energy Agency, 2014). The vast majority of these reactors are light water reactors (LWRs) with predominantly pressurized water reactors (PWRs), accounting for two thirds of the currently installed nuclear-generating capacity worldwide, followed by boiling water reactors (BWRs; Zinkle & Was, 2013; International Atomic Energy Agency, 2014). Another type of water-cooled reactors are heavy water reactors using heavy water (deuterium oxide, D_2O) as coolant and neutron moderator, which generate ~14% of the installed capacity (Zinkle & Was, 2013). In all of these water-cooled reactors, uranium oxide (UO_2) or other fissile actinide oxide powders are sintered into fuel pellets and then encased in ~4-m-long metal tubes (fuel cladding, ~1 cm outer diameter and 0.6 mm wall thickness) made of zirconium (Zr)-based alloys to form a single fuel rod. These fuel rods are grouped together into fuel assemblies that are used to build up the core of a nuclear power reactor. The core of a reactor usually consists of several hundred fuel assemblies depending on the type of reactor. Figure 1 shows the schematic view of a PWR fuel assembly from Mitsubishi Nuclear Fuel as an example (Mitsubishi). Zr alloys are also used as other fuel assembly structural components like grid spacers in PWRs and channel boxes in BWRs. The heat released by the uranium fission reaction is picked up and transported by the coolant water flowing in the primary circuit to produce electricity.

Nuclear safety is a prerequisite for the successful use of nuclear technology. The materials inside the core of a nuclear reactor are exposed to an extremely harsh environment due to the combination of high temperature, high stress, a chemically aggressive coolant, and strong radiation (Zinkle & Was, 2013). The claddings represent one of the most important components for maintaining fuel integrity and plant safety. The selection and development of Zr alloys as fuel claddings is due to their low thermal neutron absorption cross-section, reasonable corrosion performance under normal operation, and good mechanical properties under neutron irradiation (Allen et al., 2012; Terrani et al., 2014b; Motta et al., 2015). In the past decades, the emphasis of the research and development of LWR fuel was placed on improving nuclear fuel performance under normal conditions in terms of increased fuel burnup for waste minimization, increased power density for power upgrades, and extended operational service for economic competitiveness (Jeong et al., 2006; Bragg-Sitton, 2014). A new generation of advanced

***Corresponding author: Martin Steinbrueck,** Institute for Applied Materials (IAM), Karlsruhe Institute of Technology (KIT), D-76021 Karlsruhe, Germany, e-mail: martin.steinbrueck@kit.edu
Chongchong Tang, Michael Stueber and Hans Juergen Seifert: Institute for Applied Materials (IAM), Karlsruhe Institute of Technology (KIT), D-76021 Karlsruhe, Germany

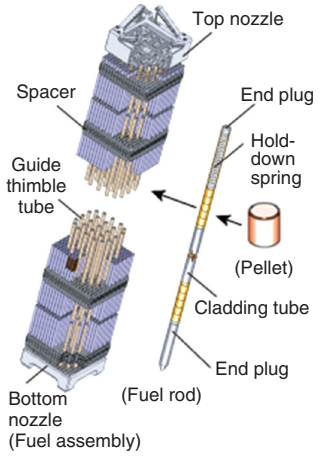

Figure 1: Schematic view of a PWR fuel assembly.

Zr-based alloy claddings, such as ZIRLO™ from Westinghouse, M5® from AREVA, and E365 for Russian reactors, has been developed, which exhibit enhanced corrosion resistance under normal conditions compared to the classical alloys Zircaloy-2 and Zircaloy-4 (Gilbon et al., 2000; Motta et al., 2015). Table 1 summarizes the composition of typical commercial Zr alloys used as claddings in water-cooled reactors. These new generation claddings with the above-mentioned improvements contribute to optimized economic operations while ensuring the safety and reliability under normal operations of nuclear power plants.

The particularly attractive properties of Zr alloy claddings make them highly suitable for normal operations (see details in Section 2); however, their satisfactory performances are highly challenged once the local environment changes from normal operating conditions to design-basis (DB) or beyond DB (BDB) accident scenarios. One recent example was the severe nuclear accident in March 2011 at the Fukushima Daiichi Nuclear Power Plant. A great earthquake of magnitude 9.0 with a subsequent 15-m tsunami seriously damaged the reactors and disabled the emergency power supply, leading to the loss of active cooling in the core (Hirano et al., 2012). The decay heat resulted in rapid temperature increase in the reactor cores and converted the coolant water into steam. Zr alloy claddings undergo severe degradation due to the rapid reaction with high-temperature steam accompanied by the generation of a large amount of heat and hydrogen. The heat generated from the steam oxidation accelerates the rising of the temperature and the meltdown of the core. The by-product hydrogen gas eventually resulted in the damage of the containment buildings through detonations with the release of highly radioactive fission products into the environment. The accidents highlighted the inherent weakness of Zr-based alloy claddings that undergo self-catalytic exothermic oxidation reaction with high-temperature steam under the loss of cooling accident conditions, which can further exacerbate both the accidents and the consequences.

Table 1: Typical commercial Zr-based alloys used as claddings in water-cooled reactors.

Alloy	Nominal alloy composition (wt.%)						
	Sn	Nb	Fe	Cr	Ni	O	Zr
Zircaloy-2	1.5	–	0.15	0.1	0.05	0.1	Bal.
Zircaloy-4	1.5	–	0.2	0.1	–	–	Bal.
ZIRLO™	1.0	1.0	0.1	–	–	0.1	Bal.
M5®	–	1.0	–	–	–	0.14	Bal.
E365	1.2	1.0	0.35	–	–	–	Bal.

Mainly after this nuclear accident, the concept of accident-tolerant fuels (ATF) has been proposed and widely investigated. By definition, ATF materials should tolerate the loss of active cooling in the core for a considerably longer period of time and up to higher temperatures than the current UO_2/Zr-based cladding fuel system that offers improved coping time under accident conditions while maintaining or improving fuel performance during normal operations (Bragg-Sitton, 2014). In terms of nuclear claddings, one key requirement is reduced oxidation kinetics with high-temperature steam and hence significantly reduced heat and hydrogen generation (Bragg-Sitton, 2014; Zinkle et al., 2014). Two primary strategies are being developed and evaluated worldwide. One approach is developing oxidation-resistant monolithic or layered cladding materials, such as iron (Fe)-based alloys, SiC composites, MAX phase materials, and multilayer molybdenum (Mo) cladding (Azevedo, 2011; Bragg-Sitton, 2014). These new cladding concepts represent a long-term strategy that requires significant engineering redesign to the cores. Another obvious and more near-term approach could be the modification of the surface of existing and available Zr alloy claddings, typically by protective coatings, to improve the oxidation resistance, as it does not significantly alter the existing UO_2/Zr-based alloy cladding fuel design.

Conventional surface modification techniques, such as ion implantation and plasma electrolytic oxidation, have been intensively investigated before to modify the surface chemistry and microstructure of Zr alloys (Sridharan et al., 2007; Hui et al., 2011). The utilization of coatings to protect structural materials, such as superalloys, refractory metals, and carbon composites, from fast oxidation to improve the service life of components at

elevated temperature always remains an important issue (Westwood et al., 1996; Padture et al., 2002). Protective coatings also have been used extensively in the nuclear industry to protect the facilities and equipment against corrosion and contamination by radioactive nuclide (ASTM Standards, 2000). However, the application of coatings on Zr alloy claddings as ATFs will obviously require much more stringent technical specifications and performance requirements. In this review, the behavior of Zr alloy claddings under normal and accident conditions is first briefly reviewed. The emphasis is placed on the most important basic coating concepts being investigated for nuclear application and their current status. Some information concerning the surface modification of Zr alloys intended for nuclear application are also included. The requirements and challenges of using coatings on Zr-based alloy claddings as ATFs are finally discussed. Due to the highly dynamic development of the research topic presented here and the numerous papers published every month, this paper will provide only representative data and references published until the end of 2016.

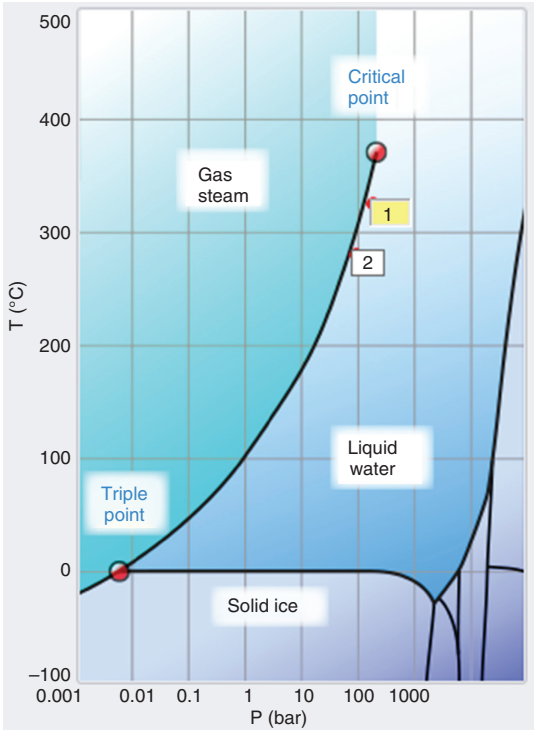

Figure 2: Phase diagram of water.
Point 1: ~330°C, 15.5 MPa (PWR condition); point 2: ~285°C, 7.5 MPa (BWR condition).

2 General overview of Zr-based alloy claddings under normal and accident conditions

Liquid water is used as the coolant in both PWR and BWR. Figure 2 shows the phase diagram of water with two points representing the normal operating conditions of PWR and BWR, respectively (Sanz et al., 2004). The operating temperatures and pressures in the core are ~330°C and 15.5 MPa for PWR and 285°C and 7.5 MPa for BWR (Zinkle & Was, 2013). The water chemistry is optimized by minor additives to ensure reliable reactor fuel performance as well as to minimize corrosion-related issues (Allen et al., 2012). The water is in subcritical state due to the combination of high temperature and high pressure and acts as a highly corrosive medium. Above the critical point (374°C, 22 MPa), the water is in supercritical state.

The waterside corrosion of Zr alloys during normal operations leads to the growth of a thin oxide scale on the surface. The weight gain kinetics usually falls into two stages, generally referred to as pretransition and posttransition, respectively. A thin, black, adherent oxide scale composed of microcrystalline grains forms initially during the pretransition period and the kinetics follows a cubic growth law governed by the diffusion of oxidizing species through the oxide (Nechaev, 1993; Allen et al., 2012). Compressive stresses are produced and accumulated within the oxide scale because of the imperfect accommodation of the molar volume expansion of the oxide to the metal from which it forms (i.e. Pilling-Bedworth ratio ZrO_2:Zr = 1.56). Once the oxide scale exceeds a certain critical thickness (usually 2–3 μm), the growth kinetics increases to a posttransition rather linear rate associated with fracture or the cracking of the oxide scale containing large amounts of porosity (Allen et al., 2012). The thickness of the oxide scale finally reaches tens of micrometers at the end of fuel cycle (Motta et al., 2015).

An additional concern associated with Zr alloys during normal operations is hydrogen pickup. Hydrogen can be produced by the cladding corrosion or by the radiolysis of water. A fraction of the hydrogen ions (protons) penetrates the oxide scale and is dissolved in the metallic matrix. It precipitates as brittle hydrides (ZrH_x) once the content exceeds the solubility limit, leading to the reduction of ductility and toughness of the cladding tube (Allen et al., 2012). This effect can significantly reduce the cladding performance during accident circumstances.

The behavior of Zr alloy claddings under DB or BDB accident scenarios, typically initiated by a loss of coolant accident (LOCA) and eventually leading to depressurization in the core and exposure to a high-temperature steam

or air environment, has been widely investigated as well (Moalem & Olander, 1991; Schanz et al., 2004; Brachet et al., 2009; Steinbrück et al., 2010, 2011). The decay heat and the stored energy rapidly drive up the core temperature. The Zr-based claddings are oxidized by the high-temperature steam and undergo ballooning and burst in the temperature range of 700°C–1200°C (Zinkle et al., 2014). In the case of DB LOCA, the emergency core cooling systems (ECCS) activates and quenches the fuel by injecting coolant water into the core. The peak clad temperature should be limited to 1204°C and equivalent cladding reacted (ECR) to 17% of the initial cladding thickness according to the US regulatory to avoid severe degradation (NRC). In terms of BDB accident scenarios with the failure of the ECCS, the Zr alloy claddings will show accelerated oxidation at temperatures above 1200°C as explained before. The oxide scale formed during normal operations also has been found to be not or weakly beneficial for the protection of underneath metallic matrix when exposed to high-temperature steam (Van Uffelen et al., 2010). The oxidation kinetics of high-temperature steam oxidation of Zircaloy can be described, for example, by a parabolic law by the following equation developed by Cathcart et al. (1977):

$$W = 601.8t^{0.5}\exp(-10050/T) \quad (1)$$

where W is the mass gain per unit surface (mg/cm^2), t is the time in seconds, and T is the temperature in Kelvin (Cathcart et al., 1977; Van Uffelen et al., 2010). The oxidation results in the formation of an outer ZrO_2 layer with an inner oxygen-stabilized α-Zr(O) layer before being completely consumed. The overall reaction of Zr with steam can be written in a simplified equation:

$$Zr + 2H_2O(g) = ZrO_2 + 2H_2(g),\ \Delta H = -584.5\ \text{kJ/mol}\ (1200°C) \quad (2)$$

3 Overview of surface modification and different types of coatings for Zr-based alloy claddings

Surface modifications by specific technologies and various types of coatings have been adopted to treat the surface of Zr-based alloys. The scientific literature on this issue was searched until the end of 2016. The surface treatments can be divided into the following categories: (A) surface modification by ion implantation, (B) nonmetallic or metallic coatings, (C) ceramic coatings including oxides, carbides, and nitrides, and (D) composite or multilayer coatings. The majority of the researches were conducted after the Fukushima accidents; few studies before the Fukushima accidents focused on improving the performance under normal conditions that aimed to withstand higher burnup. Table 2 summarizes the key features of the different types of coatings for Zr alloys as ATF claddings. The coating materials, the deposition technology, and the coating thickness are included. Furthermore, the emphasis is placed on their performances under normal operations and under accident high-temperature steam and/or air environment.

3.1 Surface modification by ion implantation

Ion implantation is a surface modification technique by which the ions of a material are accelerated to high energy and injected into a solid. Ion implantation is a low-temperature process with the advantages of no associated dimensional changes in the workpiece and the precise control of implantation profile (Conrad et al., 1987). It has been used to improve the surface properties, such as wear, corrosion, and oxidation resistance, without changing the desirable bulk properties of materials (Conrad et al., 1987). Sridharan et al. (2007) modified the surface of Zircaloy-2 alloys using the plasma immersion ion implantation of nitrogen, oxygen, and carbon and investigated their influence on the corrosion resistance in high-temperature water. The implantation depths were ~0.12 μm. The oxygen-affected layers after exposure to subcritical water (300°C) and supercritical water (500°C) at 25 MPa for 168 h for untreated and treated samples were quite similar, slightly thinner or thicker. Peng et al. (2006) examined the beneficial effect of aluminum (Al) ion implantation on the oxidation behavior of ZIRLO™ alloy at 500°C for 2 h in air. The oxidization resistance of treated samples was improved and the mass gain was reduced gradually with the increasing fluence as shown in Figure 3. However, the examined oxidation temperature was too low for ATF application.

3.2 Nonmetallic coatings

Carbon-based materials have been used as a protective layer for various nuclear applications due to excellent material properties such as high thermal stability, thermal conductivity, and low neutron cross-section (see Table 3). Pyrolytic carbon (Abdelrazek et al., 1997) and polycrystalline diamond (PCD; Skarohlíd et al., 2014; Ashcheulov et al., 2015) have been deposited using thermal cracking and microwave plasma-enhanced chemical vapor deposition (CVD), respectively, on Zr alloy fuel cladding tubes,

Table 2: Summary of different types and performances of coatings for Zr-based alloys.

Type	Coating materials	Deposition methods	Thickness	Autoclave test	Steam/air oxidation test	Performance remarks (uncoated samples as benchmark)	References
Surface modification	N, C, O	Ion implantation	~0.12 μm	300, 500°C-25 MPa-168 h	–	Comparable oxide layer thickness after corrosion	Sridharan et al., 2007
	Al	Ion implantation	~0.30 μm	–	500°C-air-2 h	Reduced mass gain with increasing implantation fluence, maximum reaching 30% of the untreated sample	Peng et al., 2006
Nonmetallic	Pyrolytic carbon	Thermal cracking	–	–	–	Technological parameters for the preparation investigated, low coating rate	Abdelrazek et al., 1997
	PCD	CVD	~0.30 μm	–	950–1100°C-steam-30 min	Slightly improved steam oxidation resistance; stability after short time ion irradiation (10 dpa, 5 h, 3 MeV Fe^{2+})	Skarohlíd et al., 2014; Ashcheulov et al., 2015
	Si	PS+LBS	70–120 μm	–	1200°C-steam-2000 s	Improved oxidation resistance	Kim et al., 2014
	$ZrSi_2$	Sputtering	~0.85 μm	–	700°C-air-5 h	33% reduction in weight gain	Hwasung et al., 2016
Metallic	Sn	Evaporation	0.02–0.23 μm	349°C-17.6 MPa-63 days	500°C-air, 403°C-steam, 80 days	Slightly improved resistance under both autoclave and oxidation test with coating thickness up to 0.1 μm	Hauffe, 1976
	Y	Sputtering+heavy ion bombardment	~0.1 μm	400°C-25 MPa-168 h	–	Improved corrosion resistance	Sridharan et al., 2007
	Cr	PVD	5–30 μm	360°C, 415°C-10 MPa-200 days	Up to 1300°C-steam	Excellent corrosion resistance (tens of times lower) and reduced hydrogen pickup under normal conditions	Brachet et al., 2015; Idarraga-Trujillo et al., 2013
		Cathodic arc evaporation	~4 μm	360°C-18 MPa-1000 h	1100°C-steam-4 h	Significant improved high-temperature steam oxidation resistance up to 1200°C	Ivanova et al., 2013
		PS+LBS	80 μm	–	1200°C-steam-2000 s		Kim et al. 2013
		Arc ion plating	~10 μm	–	1200°C-steam-2000 s	Negligible reduction of residual strength and ductility before the completely consumption of the metallic Cr layer	Park et al., 2015
		3D laser coating/cold spraying	80–200 μm	360°C-18.9 MPa-15 days	1200°C-steam-3000 s	Improved ballooning and rupture resistance	Kim et al., 2016; Park et al., 2016
	Al-Zr	Magnetron sputtering+thermal annealing	~1 μm	–	800–1000°C-steam-2 h	AlZr intermetallic formation; improved oxidation resistance at 800°C, no protective effect at 1000°C	Carr et al., 2016
	Ni-Zr	Electroplating+thermal treatments	2.5–10 μm	–	290–370°C-steam-64 days	Thick coating cracked after annealing, NiZr intermetallic formation; too low oxidation temperatures	Luscher et al., 2013

Table 2 (continued)

Type	Coating materials	Deposition methods	Thickness	Autoclave test	Steam/air oxidation test	Performance remarks (uncoated samples as benchmark)	References
	FeCrAl alloy and 310 steel	HIP of Zr powder inside cans	~2 mm	–	Up to 1300°C-steam	Brittle intermetallic formed; improved oxidation resistance but too thick coatings; eutectic in binary Fe-Zr at ~900°C	Terrani et al., 2013
	FeCrAl alloy	PVD	0.3–1.1 μm	288°C-9.5 MPa-20 days	700–1100°C-steam-10 h	$NiFe_2O_4$ spinel formation under normal BWR condition, two times higher mass gain; significantly reduced oxidation resistance with high Al content during steam exposure	Zhong et al., 2016
Oxide	Al_2O_3	Magnetron sputtering or electron beam evaporation + oxidation	~1 μm	350°C-20 MPa-24 h	–	Unstable, soluble, and transform to AlOOH during normal conditions	Baney & Tulenko, 2003
	ZrO_2	Plasma electrolytic oxidation	30 μm	500°C-25 MPa-500 h	–	Better corrosion resistance in static autoclave, similar weight changes in a flowing system	Hui et al., 2011
Carbide	SiC	Pulsed plasma enhanced CVD (PE-CVD)	~1 μm	350°C-20 MPa-24 h	1200°C-steam	Unstable, soluble during autoclave test; little improvement during steam oxidation	Baney & Tulenko, 2003; Al-Olayyan et al., 2005
	Ti_2AlC	Cold spray or HVOF process	40 μm	–	1200°C-steam	Composition change during HVOF; loose structure with pores and impurities; poor performance and fast oxidized	Pantano et al., 2014
		Cold spray	~90 μm	–	700, 1005°C-steam-60 min	High hardness and wear resistance, relatively dense structure, significantly improved oxidation resistance	Maier et al., 2015
		Magnetron sputtering + thermal annealing (800°C)	~5 μm	–	800–1200°C-steam-4 h	Dense and phase-pure coatings, protective alumina scale formed at 800°C, little improvement as temperature exceeded 1000°C, thick coating needed	Tang et al., 2016
		Magnetron sputtering + laser surface annealing (900°C)	1–5 μm	400°C-10.3 MPa-72 h	–	Formation of microcracks after laser treatment; protective effect shown during autoclave test	Yeom et al., 2016
	Cr_2AlC	Magnetron sputtering + thermal annealing	~1 μm	360°C-18.6 MPa-10 days	–	Partial spallation observed after autoclave test, improved corrosion resistance for coated area	Roberts, 2016
Nitride	TiN	PVD	4 μm	–	–	Improved friction and wear damage resistance	Sung et al., 2001
	TiN and TiAlN	Pulsed laser deposition (PLD)	~2 μm	500°C-25 MPa-48 h	–	Significant improved corrosion resistance, better performance of TiN coatings	Khatkhatay et al., 2014

Table 2 (continued)

Type	Coating materials	Deposition methods	Thickness	Autoclave test	Steam/air oxidation test	Performance remarks (uncoated samples as benchmark)	References
	TiN and TiAlN	Vacuum cathodic arc evaporation	4–12 μm	360°C-18.7 MPa-3 days	–	Excellent corrosion resistance of TiN coatings, poor performance of TiAlN coatings due to the formation of AlOOH	Alat et al., 2015
	CrN, CrAlN, and TiAlN	PVD	2–4.5 μm	350°C-16.5 MPa-30 days	1000–1100°C-steam-15 min	Excellent corrosion resistance and reduced steam oxidation of CrN coatings, unstable of CrAlN and TiAlN coatings during autoclave tests; reduced hydrogen ingress	Nieuwenhove et al., 2015
Composite/ multilayer	Cr_3C_2 + NiCr	HVOF process	250 μm	400°C-10.3 MPa-3 days	700–1000°C-steam/air-60 min	Loose structure of the coatings, higher mass gain during autoclave test, reduced steam oxidation rate	Jin et al., 2016
	Mo/FeCrAl	Cold spraying	15 + 200 μm	-	1200°C-steam-3000 s	Negligible interdiffusion between the coating and the substrate and oxidation after test; 1.17 mm interdiffusion layer generated for coatings without barrier	Park et al., 2016
	Al/amorphous alumina	Electron beam evaporation + sputtering	~1 μm	343°C-20.1 MPa-200 days	–	Unstable, dissolve of the coatings during autoclave test	Park, 2004
	CrZr/Cr/CrN	Vacuum cathodic arc evaporation	~7 μm	–	600–1100°C-air-60 min	Several times decreased oxidation rate	Kuprin et al., 2014, 2015
	Alternating TiN/Ti	Reactive evaporation	1–4 μm	360°C-22 MPa-200 days	–	Greatly improved corrosion and hydriding properties of Zircaloy; large number of sublayers preferred for optimal performance	Wiklund et al., 1996
	Alternating Cr/CrAl	Vacuum cathodic arc evaporation	~4 μm	360°C-18 MPa-1000 h	1100°C-steam-4 h	Around 10 times decreased corrosion rate and several times decreased oxidation rate	Ivanova et al., 2013
	Alternating TiAlN/TiN	Vacuum cathodic arc evaporation	8–12 μm	360°C-18.7 MPa-90 days	–	Significantly improved corrosion resistance for coatings with more sublayers	Alat et al., 2016

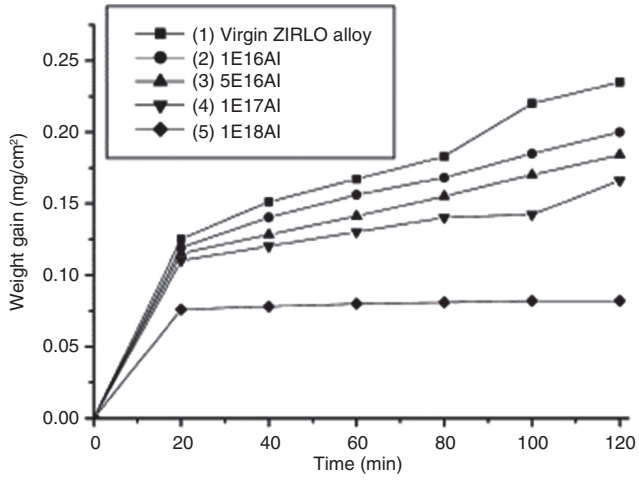

Figure 3: Oxidation curve of ZIRLO alloy implanted with Al fluences from 0 to 10^{18} ion/cm^2 at 500°C in air.
Reproduced from Peng et al. (2006) with permission from Elsevier.

aiming to mitigate the pellet cladding interaction-stress corrosion cracking (PCI-SCC) problem and to improve the accident tolerance. Pyrolytic carbon coating was produced by the thermal cracking of commercial butane gas to coat the inner surface of Zircaloy-4 tubes. Both coatings could be grown at relatively low temperature but with quite low growth rate (~20 nm/h at 450°C for PCD coatings). For pyrolytic carbon coatings, the deposition process was investigated to yield high efficiency and no corrosion or oxidation tests were conducted. Concerning PCD coatings, the oxidation resistance was slightly improved in high-temperature steam, and the weight gain of PCD-coated Zircaloy-2 (0.20 g/dm^2) was lower than that of the unprotected Zircaloy-2 sample (0.38 g/dm^2) after oxidation at 950°C steam for 30 min. The PCD films could maintain structural integrity after short-time ion beam irradiation (10 dpa, 5 h, 3 MeV Fe^{2+}). The performance under normal operations needs to be further investigated.

Another interesting nonmetallic coating is silicon (Si)-based material, as an SiO_2 scale represents one of the most effective barriers against high-temperature oxidation. Kim et al. (2014) deposited Si coatings on Zircaloy-4 using plasma spray (PS) or laser beam scanning (LBS) treatment after the PS (PS + LBS) process. The thickness of the Si coating layer depends on the repeated spraying passes. The mean thickness of the Si layer was ~15 μm for one pass, and the variation of the thickness was ~3 μm. Thus, a uniform-layer thickness cannot be obtained by a one-pass PS treatment. Pores of irregular shape were observed in the Si coating layers as shown in Figure 4A, and the density of pores was increased with increasing repeated spraying passes. After LBS treatment, the coatings became much denser, showing better adherence due to the formation of an Si-Zr mixed layer (Figure 4A, right). Figure 4B shows the oxidation rate of Si-coated Zircaloy-4 sheets in a steam environment at 1200°C for 2000 s. The oxidation resistance of the Si coating is somewhat improved relative to that of the Zircaloy-4 sheet. The authors claimed that severe oxidation progressed at the interface region between the PS Si layer without treatment and Zircaloy-4 substrate, which grew along the pore network formed in the PS Si coating layer. However, the PS + LBS-treated Si-coated samples showed superior oxidation resistance than that of bare

Table 3: Summary of the various properties for primary elements as coating components.

Element	Thermal neutron absorption cross-section (Barns)	Density	Melting point (°C)	Thermal expansion (×10^{-6} K^{-1}, RT)	Thermal conductivity W/(m K), RT
C	0.003	2.26	3650 (sublimation)	0.6–4.3	129
N	1.88	–	–	–	–
O	0.0001	–	–	–	–
Al	0.22	2.70	660	23.2	237
Si	0.13	2.33	1410	2.6	148
Ti	5.6	4.51	1670	7.1	22
Cr	2.9	7.14	1850	6.7	94
Fe	2.4	7.87	1539	11.5	80
Ni	4.5	8.91	1455	13.3	91
Y	1.28	4.47	1526	10.6	17
Zr	0.18	6.51	1845	5.8	23
Nb	1.1	8.57	2415	7.2	54
Sn	0.63	7.31	232	22	67
Mo	2.48	10.28	2617	6.0	138

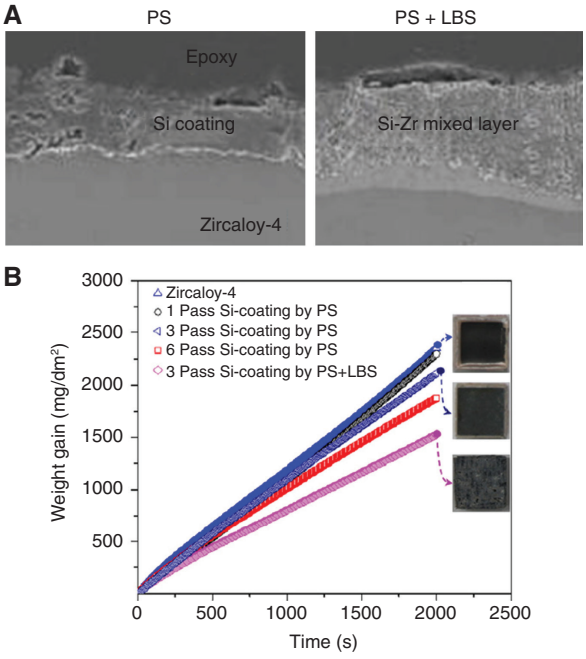

Figure 4: Cross-sectional scanning electron microscopy (SEM) observation of Si coatings on Zircaloy-4 prepared by PS and PS + LBS (A) and oxidation rate of Si-coated Zircaloy-4 sheets in a steam environment at 1200°C for 2000 s (B).
Reproduced from Kim et al. (2014) with permission from ASTM International.

Zircaloy-4 after exposure to 1200°C steam for 2000 s (Figure 4B). The Zircaloy microstructure at the coating-substrate interface was changed by a laser heat source and the modified phase thickness significantly depended on the process parameters.

Amorphous $ZrSi_2$ thin-film coatings (850 nm) were successfully deposited on Zircaloy-4 alloy without any significant defects by sputtering (Hwasung et al., 2016). The coated samples demonstrated a 33% reduction in weight gain after oxidation in air at 750°C for 5 h compared to the uncoated Zircaloy-4. The scale after oxidation consisted of both SiO_2 and ZrO_2.

3.3 Metallic coatings

3.3.1 Pure element coatings

Tin-coated Zircaloy-4 samples with different coating thicknesses up to 0.23 μm were prepared by evaporation under vacuum (Hauffe, 1976). The high-pressure water corrosion rate at 349°C and 17.6 MPa and oxidation rate in argon (Ar)-oxygen mixture with 33 kPa oxygen pressure at 500°C were slightly decreased with increasing thickness of the tin layer (up to 0.1 μm). This improvement presumably was caused by the tin layer that existed as a liquid agent between the alloy and the oxide as discussed by the authors.

A thin yttrium layer was deposited on Zircaloy-2 by sputtering (Sridharan et al., 2007). After deposition, the coating was ion bombarded using Xe^+ ions to improve film adhesion. The treated samples showed better corrosion resistance, only a thin oxygen diffusion layer on the surface, after exposure at 400°C and 25 MPa water for 168 h compared to that of untreated one. The enhanced oxidation resistance possibly was attributed to the formation of a mixture of ZrO_2 and Y_2O_3 scale.

Metallic chromium (Cr) has attracted much attention as a kind of coating material on Zr alloys due to its high melting point, good high-temperature oxidation resistance, and similar thermal expansion coefficient compared to Zr (see Table 3). Cr coatings on Zr-based alloy substrates fabricated by different technologies have been investigated by various institutes like Brachet et al. (2015) and Idarraga-Trujillo et al. (2013) from CEA (France) by physical vapor deposition (PVD), Ivanova et al. (2013) from Russia using vacuum arc ion-plasma technology, and Kim et al. (2013) from Korea using several different methods, such as PS with subsequent LBS, arc ion plating (Park et al., 2015), 3D laser technology (Kim et al., 2016), and cold spraying (Park et al., 2016). The primary advantages of selecting Cr as coating material are based on the formation of a protective Cr_2O_3 scale on the surface during corrosion and oxidation. The Cr_2O_3 scale has been proven stable under normal conditions in autoclave tests as it acts as a diffusion barrier. After exposure at 415°C and 10 MPa for 200 days, the mass gain was lower than 0.05 mg/cm² for Cr-coated Zircaloy-4 sample deposited by PVD, corresponding to an outer Cr oxide thickness lower than 250 nm, which was ~50 times lower than that on uncoated samples (Brachet et al., 2015). In addition, the Cr coatings can provide significant additional margins for LOCA (<1200°C) and, to some extent, for BDB conditions as shown in Figure 5. The Cr coating deposited by PVD displays a columnar morphology with a fully dense microstructure free of defects (Figure 5A). A protective Cr_2O_3 scale formed on the surface after oxidation at 1200°C in steam for 300 s for Cr-coated sample (Figure 5B). The formation of a thick brittle outer ZrO_2 layer and an inner α-Zr(O) layer was confirmed for uncoated Zircaloy-4 samples after oxidation at the same conditions (Figure 5C). The Cr-coated samples also demonstrated negligible reduction of residual strength and ductility (Figure 5D) before the complete consumption of the metallic Cr layer (Brachet et al., 2015) and improved ballooning and rupture resistance (Park et al., 2016). The amount of hydrogen picked up by the cladding was

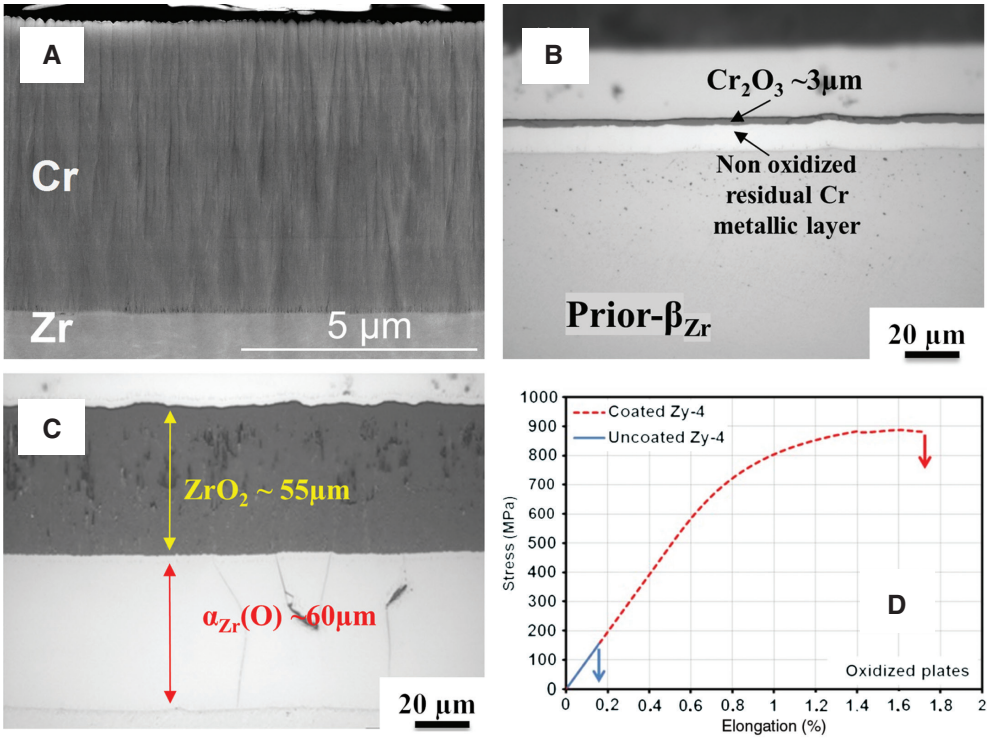

Figure 5: Cr coating deposited by PVD (A) and oxide scales of Cr-coated (B) versus uncoated Zircaloy-4 (C) samples after oxidation at 1200°C for 300 s in steam; (D) tensile stress-strain curves obtained at RT on uncoated and coated Zircaloy-4 after two-side steam oxidation for 15,000 s at 1000°C.
Reproduced from Brachet et al. (2015) with permission from the author.

significantly reduced simultaneously due to the existence of a Cr_2O_3 barrier.

Figure 6 summarizes the corrosion and oxidation rates in PWR simulating pressurized water (360°C, ~18 MPa) and in high-temperature steam at 1200°C during LOCA conditions, respectively, of uncoated and Cr-coated Zr-based alloys fabricated by different processes. In general, metallic Cr and Cr-coated Zr alloys show superior corrosion resistance with by one magnitude lower weight gain than uncoated Zr-based alloys. Excellent corrosion resistance for Cr-coated Zr alloys fabricated by various deposition techniques during autoclave tests also has been proven (Figure 6A). Regarding the high-temperature steam oxidation tests at 1200°C, improved oxidation resistance can be seen for Cr-coated samples as shown in Figure 6B; the weight gains were several times lower for coated samples. It is necessary to mention that coatings deposited by PVD, although much thinner, seem to

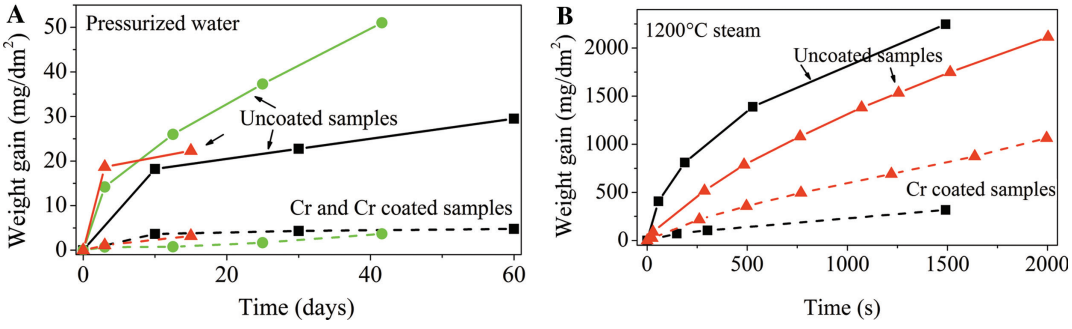

Figure 6: Comparison of corrosion rate in PWR simulating pressurized water (A) and high-temperature steam oxidation rate during LOCA conditions (B) of uncoated and Cr-coated Zr-based alloys fabricated by different processes.
■, Cr coatings deposited by PVD (Brachet et al., 2015); ▲, Cr coatings deposited by spraying (Kim et al., 2016; Park et al., 2016); ●, Cr coatings deposited by cathodic arc evaporation (Idarraga-Trujillo et al., 2013).

perform better than those deposited by spraying due to the denser structure.

Brachet et al. (2015) also investigated the impact of preexisting defects (i.e. cracks in as-deposited samples) on the performance of the coatings under normal and accident conditions. Figure 7 shows the optical micrographs of Cr-coated Zircaloy-4 sheet samples after autoclave test at 360°C for 60 days and then oxidation at 1100°C in steam for 850 s (Brachet et al., 2015). The results illustrated that the coatings showed certain self-healing features, and the cracks have only a limited and localized impact on the overall oxidation of the coated sample under the test conditions. No spallation of the coatings and accelerated oxidation of the underneath Zircaloy was observed.

Kim et al. (2016) performed ring compression and ring tensile tests to evaluate the adhesion properties between the Cr-coated layer by 3D laser technology and the Zr-based alloy tube at room temperature (RT). Figure 8 shows the ring tensile test results and sample appearance of the Cr-coated Zircaloy-4 cladding tube after the test. The thickness of the Cr-coated layer ranged from 80 to 200 μm. The Cr-coated layer was free of defects up to 4% strain with somewhat increased strength, whereas the lateral cracks were formed in the Cr-coated layer after 6% strain. Nevertheless, the interface between the Cr-coated layer and Zircaloy-4 substrate was maintained without peeling (Kim et al., 2016).

For Cr coating deposited by cold spraying, posttreatment by cold rolling was adopted to reduce the undesirable high surface roughness and defects in the coated layer. The coated Zr plate samples showed no significant cracking or spallation of the coated layer despite a reduction

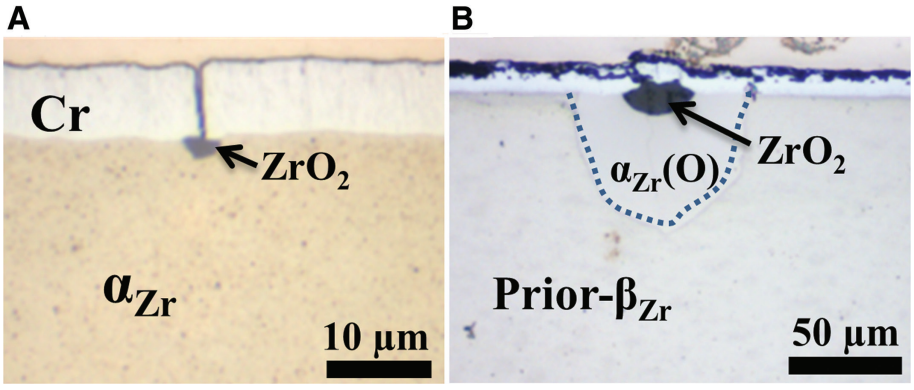

Figure 7: Optical micrographs of Cr-coated Zircaloy-4 samples with a preexisting crack throughout the coating thickness after autoclave test at 360°C for 60 days (A) and then oxidation at 1100°C in steam for 850 s (B).
Reproduced from Brachet et al. (2015) with permission from the author.

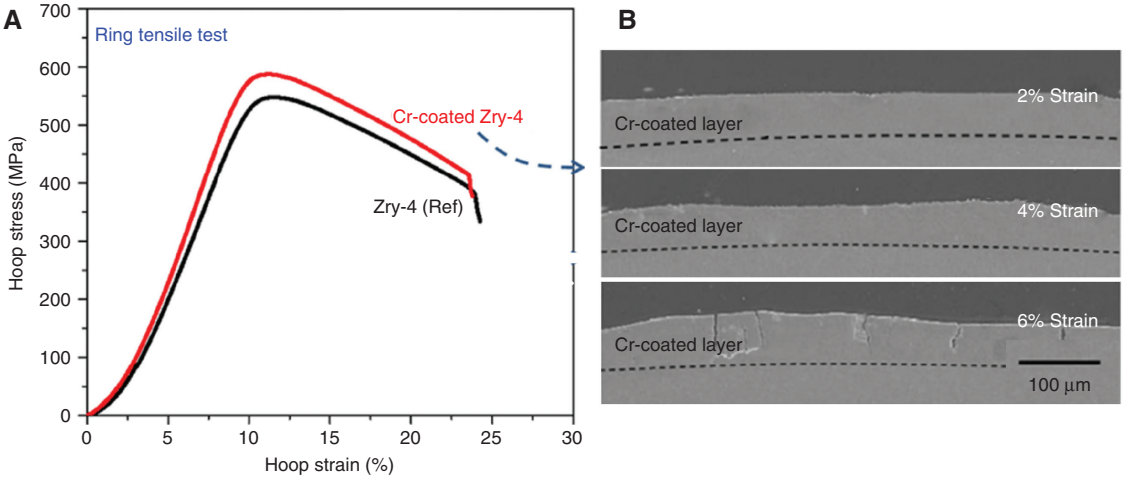

Figure 8: Ring tensile test result (A) and cross-sectional SEM observation of Cr-coated Zircaloy-4 cladding tubes deposited by 3D laser technology after the ring tensile tests at 2%, 4%, and 6% strain (B).
Reproduced from Kim et al. (2016) with permission from Elsevier.

to ~55% of the original thickness after cold rolling with significantly reduced roughness and defects. However, it is well known that pure Cr is extremely brittle at RT (Gu et al., 2004). The cold rolling treatment probably induces the stress concentration within the coatings and makes the coatings susceptible to degrade during service. In addition, the plate samples after being cold rolled showed uneven interface between the coated layers and Zr matrix and thickness variation in the coated layers. Further studies should be conducted to determine the feasibility of this process for fabricating coated claddings (Park et al., 2016).

3.3.2 Intermetallic coatings

Carr et al. (2016) prepared Al-modified Zircaloy surfaces by magnetron sputtering of Al and subsequent thermal annealing in vacuum at 823 K for 2 h. The formation of Al-Zr intermetallic phases within the coatings and Al-rich clusters on the surface was observed after annealing. The Al-doped specimens demonstrated better oxidation behavior at 800°C in steam for 120 min with average oxide layer thicknesses of ~0.7 μm (~8 μm for undoped specimens). However, the oxide layer was even slightly thicker for treated specimens after oxidation at 1000°C.

The surfaces of Zircaloy-4 substrates were modified with nickel (Ni)-Zr (NiZr) intermetallics by electroplating with Ni followed by thermal treatment at ~760°C (Luscher et al., 2013). A series of brittle intermetallic phases formed at surfaces rich of Ni; the 10-μm-thick coatings cracked after annealing. The coated samples were oxidized at 290°C to 370°C in steam under a constant partial pressure of oxidant (1 kPa D_2O in dry Ar at 101 kPa) for 64 days. The coated samples demonstrated initially enhanced oxidation rate until the coatings became oxygen saturated compared to that of bare Zircaloy-4 substrate. However, the testing temperatures were quite low even for DB accident conditions.

3.3.3 Alloy coatings

Other interesting metallic coating materials for Zr-based claddings are Fe-based alloys, especially FeCrAl alloys, which have shown quite good corrosion resistance under normal conditions and excellent high-temperature steam oxidation resistance due to the formation of a protective alumina scale. Terrani et al. (2013) produced outer layers of FeCrAl ferritic alloy and type 310 austenitic stainless steel on the surface of Zr metal slugs by hot isostatic pressing (HIP) of Zr powder inside cans (2 mm thick). The FeCrAl layer experienced less degradation and could protect the Zr up to 1300°C for 8 h. The primary degradation mechanism for the protective layer at 1300°C was interdiffusion with the Zr (several hundred microns thick intermetallic diffusion layer).

Zhong et al. (2016) deposited FeCrAl films of varying composition on Zircaloy-2 by magnetron sputtering. These films containing Al concentration of 18 at.% or higher, which promoted alumina formation, significantly reduced the oxidation rate during 700°C steam exposure. Fe-Zr eutectic reaction, which was observed at ~900°C (Zr_3Fe), resulted in the fast degradation of the film when the oxidation temperatures exceeded 900°C as observed before. Therefore, a proper stable diffusion barrier needs to be developed. Autoclave tests under normal BWR operating conditions at 288°C and 9.5 MPa with normal water chemistry (2 ppm dissolved oxygen) up to 20 days were also conducted to examine the performance of the FeCrAl coatings. The formation of an $NiFe_2O_4$ spinel on the surface after exposure was observed due to testing in an Ni-based alloy autoclave; however, the coated specimens indicated greater corrosion product with higher mass gain by a factor of ~2 at 20 days compared to the uncoated specimens. Overall, the FeCrAl films demonstrated sufficient performance without loss of integrity after 20 days of exposure.

3.4 Ceramic coatings

Different types of ceramic coatings, including oxides serving as a diffusion barrier as well as carbides and nitrides that form protective oxide layers during corrosion and oxidation, have also been examined to improve the performances of Zr-based claddings.

3.4.1 Oxide coatings

Alumina coatings (1 μm thick) were prepared on Zircaloy-4 substrates using radiofrequency sputtering or electron beam evaporation followed by tailored oxidation at low temperature (Baney & Tulenko, 2003). However, the alumina films have been proven to be unstable during autoclave exposure (350°C, 20 MPa) and transformed to unprotective boehmite (AlOOH). A significant solubility of the alumina in subcritical water also has been observed by other studies, whereas the alumina is proven to be insoluble and stable in supercritical water (Hui et al., 2011).

ZrO_2 coatings with 50 μm thickness and free of open pores and cracks were successfully formed on Zr-2.5Nb substrates using a plasma electrolytic oxidation method. The coated samples showed somewhat better corrosion resistance than the bare substrates when tested in static autoclaves but showed similar weight changes when tested in a flowing system in supercritical water at 500°C and 25 MPa (Hui et al., 2011).

3.4.2 Carbide coatings

Two different types of carbides, SiC as well as Ti_2AlC and Cr_2AlC MAX phases, have been investigated as protective coatings on Zr-based alloys due to their excellent high-temperature oxidation resistance as bulk materials. Olayyan and colleagues (Baney & Tulenko, 2003; Al-Olayyan et al., 2005) deposited l-μm-thick SiC coatings by plasma-assisted CVD (PACVD) on Zircaloy-4 substrate at ~370°C. They found that higher adhesion strengths of the coatings were obtained for a moderate level of substrate roughness. However, the SiC coating failed to survive and disappeared after autoclave tests at 350°C and 200 MPa for 24 h. The mechanisms of SiC film failure during autoclave exposure was probably attributed to the formation and dissolution of SiO_2 by hydrothermal corrosion, film cracking, and spallation due to various stresses.

Ti_2AlC and Cr_2AlC belong to a family of nanolaminated ternary compounds with the general formula of $M_{n+1}AX_n$ (short as MAX, n typically is 1–3). The unique structure contributes to their attractive properties combination of both ceramics and metals (Barsoum, 2000). Al-containing MAX phases, especially Ti_2AlC and Cr_2AlC, possess excellent high-temperature oxidation resistance both in air and in steam due to the formation of a dense and adherent alumina scale (Tallman et al., 2013). Various deposition processes, including high-velocity oxygen fuel (HVOF) process (Pantano et al., 2014), cold spray (Maier et al., 2015), and magnetron sputtering followed by thermal (Tang et al., 2016) or laser annealing (Yeom et al., 2016) in Ar or vacuum, have been adopted to produce Ti_2AlC coatings on Zr-based alloys. In general, HVOF and cold-spray processes can produce relatively thick coatings up to more than 100 μm. The microstructure of such films is relatively loose with pores and the coatings also contain a significant amount of secondary phases, such as TiC and TiAl intermetallics. Deposition by magnetron sputtering can result in dense coatings with minor or no secondary phases. The coating thickness is usually limited to a few or few tens of microns. Figure 9 shows typical cross-sectional views of Ti_2AlC coatings deposited by spraying and magnetron sputtering with obviously different microstructures described above. Composition changes during deposition of Ti_2AlC coatings using the HVOF process were observed and the coatings showed poor performance during high-temperature oxidation. It was suggested that a minimum coating thickness of ~90 μm was needed for the protection of ZIRLO against oxidation at 1200°C in steam (Pantano et al., 2014). The cold spray of Ti_2AlC coatings on Zircaloy-4 with 90 μm thickness showed significantly superior steam oxidation resistance compared to the Zircaloy-4 substrate at 1005°C for short time (20 min; Maier et al., 2015). The coatings showed higher hardness and better wear resistance than uncoated Zircaloy-4. After pin-on-disk wear tests, a pronounced wear track formed on the Zircaloy-4, whereas the wear track on the MAX phase coating was minimal, indicating a higher abrasive wear resistance of the MAX phase coating. Dense and phase-pure Ti_2AlC coatings (5 μm thick) with 500 nm thickness TiC barrier were produced on Zircaloy-4

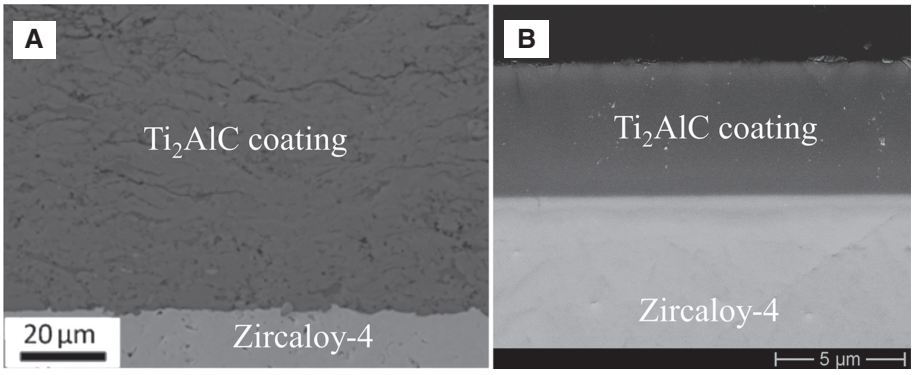

Figure 9: Typical SEM cross-sectional microstructure of Ti_2AlC coatings deposited by different processes: (A) cold spraying (Maier et al., 2015) and (B) magnetron sputtering followed by thermal annealing (Tang et al., 2016).
Reproduced with permission from Elsevier.

by magnetron sputtering followed by thermal annealing at 800°C in Ar. The coated samples have demonstrated excellent oxidation resistance at 800°C in steam. The performance was limited by the coating thickness and only slight improvement was observed once the oxidation temperature exceeded 1000°C due to the fast consumption of the coatings (Tang et al., 2016). Yeom et al. (2016) produced Ti_2AlC coatings by magnetron sputtering followed by laser surface annealing to not affect the microstructure of the Zircaloy-4 substrate. However, the formation of microcracks after laser treatment was observed.

Roberts (2016) has deposited Cr_2AlC coatings with 1 μm thickness on ZIRLO by magnetron sputtering at 550°C. After autoclave tests at 360°C and 18.6 MPa for 10 days, the coated samples showed significantly less mass gain compared to the noncoated ones. However, the partial spallation of the coatings after tests was observed. The coated area displayed better corrosion resistance than the spalled-off area and the corrosion of the coatings resulted in formation of AlOOH and Cr_2O_3.

3.4.3 Nitride coatings

Refractory metal nitrides are well known for their high hardness and melting temperatures as well as reasonable corrosion and oxidation resistance. Therefore, they are used as protective coatings in various industries (Pierson, 1996). Two main types of nitrides, titanium nitride (TiN) and CrN with sometimes additional Al incorporation, have been studied as protective coatings to improve the fretting damage or corrosion and oxidation resistance of Zr-based claddings. The fretting damage of TiN-coated Zircaloy-4 tubes showed that the wear volume of TiN-coated Zircaloy-4 tube decreased by 1.2 to three times compared to the uncoated tube and the wear mechanisms were brittle fracture of TiN before destroying the coating (Sung et al., 2001). TiN and CrN coatings exhibited excellent corrosion resistance during autoclave tests due to the formation of stable oxide scales, TiO_2 and Cr_2O_3, respectively (Khatkhatay et al., 2014; Alat et al., 2015; Nieuwenhove et al., 2015). For Al-containing coatings (i.e. TiAlN and CrAlN), the formation of AlOOH was observed during autoclave exposure, which was detrimental to corrosion performance due to its high growth rate and poor adhesion. Significant cracking and spallation of the Al-containing coatings were frequently observed during autoclave test, which led to the subsequent oxidation and recession of the coating (Alat et al., 2015; Nieuwenhove et al., 2015). Figure 10 shows an example of the formation of AlOOH on the surface of TiAlN coatings and uniform corrosion of TiN coatings after autoclave test (Alat et al., 2015). However, the performance of the coatings in high-temperature steam atmosphere was not sufficiently investigated; some limited tests showed slightly reduced oxidation rates for coated samples up to 1100°C for short exposure time.

3.5 Composite/multilayer coatings

Composite or multilayer coatings often show enhanced properties, such as hardness, adhesion, wear, and

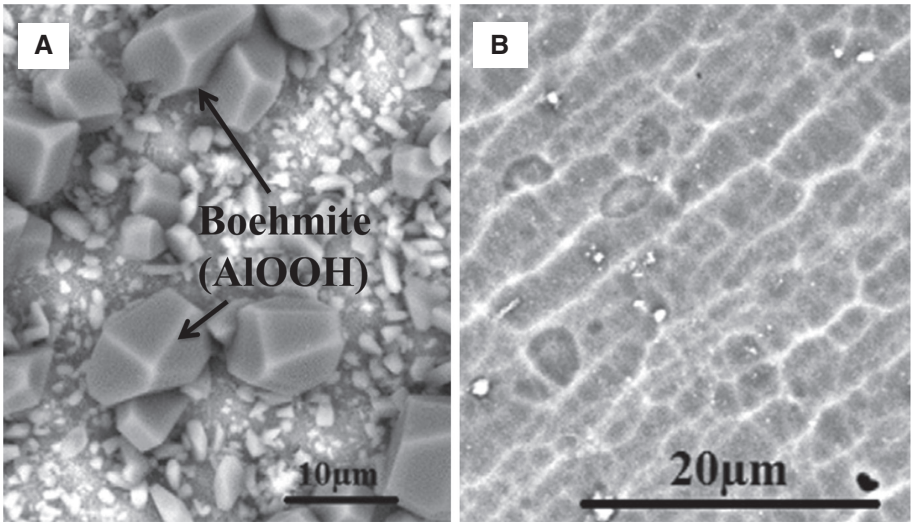

Figure 10: SEM surface view of TiAlN (A) and TiN (B) coatings after autoclave tests at 360°C and 18.7 MPa for 3 days. Reproduced from Alat et al. (2015) with permission from Elsevier.

corrosion resistance, compared to single-layer coatings (Stueber et al., 2009). Several composite or multilayer coating concepts have been investigated as ATF coatings, aiming to improve the bonding strength, to alleviate the interdiffusion or reaction between the coating and the substrate, and to suppress the propagation and expansion of various defects, such as pores and cracks, in the coatings. Another attempt is to improve the performance of the coatings by the utilization of corrosion-resistant coating as the outer layer and oxidation-resistant coating as the inner layer that can enable the coatings function during both normal and accident conditions.

Jin et al. (2016) deposited Cr_3C_2-NiCr composite coatings on Zr-2.5Nb substrates using the HVOF process. The coating thickness reached 250 μm, but the structure of the coatings was loose with many micropores. The coatings had shown good corrosion resistance during autoclave exposure; however, the Zircaloy substrate was seriously attacked due to the loose structure of the coatings. Higher mass gain was observed even for the coated samples due to the bimetallic effect. The coated samples gained slightly less weight gain during exposure to steam from 700°C to 1000°C.

Park et al. (2016) deposited an Mo layer with ~15 μm thickness between FeCrAl coating and the Zr matrix by cold spraying to prevent interdiffusion at high temperatures. The thickness of FeCrAl coatings was ~200 μm. The sample modified with this diffusion barrier showed little oxidation on the surface and negligible interdiffusion between the coating and the substrate after exposure at 1200°C for 3000 s in steam (Park et al., 2016). For the FeCrAl coatings without Mo barrier, although similar little oxidation occurred on the surface, the diffusion depth of the alloying elements from the FeCrAl coatings into the Zr matrix was more than 1.17 mm after oxidation, and as a result, intermetallic compounds were generated deep in the Zr matrix (Park et al., 2016).

Similar to the previous studies, Al-based multilayer coatings with an inner Al layer and an outer amorphous alumina layer have been further proven to be not suitable due to the instability of alumina under normal conditions in subcritical water (Park, 2004). The amorphous alumina layer was hydrothermally corroded to AlOOH with poor adherence and fast growth rate.

Multilayer Cr-Zr/Cr/CrN coatings for the protection of Zr alloys from fast steam oxidation deposited by the vacuum-arc evaporation technique were investigated by Kuprin et al. (2014, 2015). Figure 11 shows the cross-sectional microstructure of the as-deposited coatings and the coating after oxidation at 1100°C for 60 min in steam. The overall coating thickness was ~7 μm, with the Cr_2Zr layer being 4 μm, the Cr layer 0.5 μm, and the outer CrN layer 2 μm thick. The steam oxidation resulted in the growth of an oxide scale with a thickness of <5 μm for the coated samples, and some coatings remained unconsumed. The oxidation resistance was greatly improved compared to bare claddings.

In addition, the concepts of multilayer coatings with numerous alternative thin sublayers were proposed and studied. Wiklund et al. (1996) have investigated TiN/titanium (Ti) multilayers as diffusion barriers to enhance the corrosion and hydriding resistance of Zircaloy claddings under normal conditions. The coatings, including five different arrangements, were ordered stacks of TiN and Ti layers with different numbers of sublayers and individual sublayer thickness. All the coatings have demonstrated great improvement of corrosion and hydriding properties of Zircaloy after an autoclave test at 360°C and 22 MPa for 200 days. A thick multilayer coating with a large number of sublayers has been proven favorable for

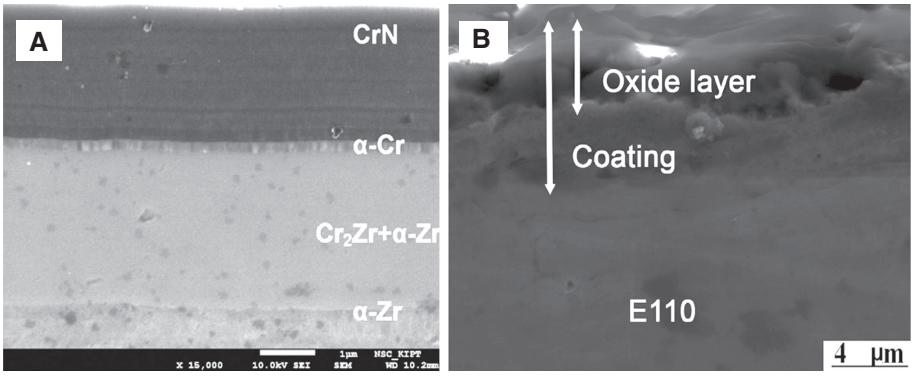

Figure 11: Cross-sectional view of multilayer Cr-Zr/Cr/CrN coatings on E110 cladding: (A) as-deposited and (B) after oxidation at 1100°C for 60 min.
Reproduced from Kuprin et al. (2015) with permission from Elsevier.

optimal performance. Recently, similar coating architectures but with Cr/CrAl (Ivanova et al., 2013) and TiAlN/TiN (Alat et al., 2016) multilayers were evaluated. The Cr/CrAl coatings deposited by vacuum arc ion-plasma evaporation with ~5 µm thickness showed ~10 times decreased corrosion rate during autoclave tests and several times decreased oxidation rate up to 1100°C in steam compared to the bare substrate (Ivanova et al., 2013). The adoption of the TiAlN/TiN multilayer architecture was aimed to avoid AlOOH phase formation with minimal weight gain under normal operating conditions as well as to form a stable Al_2O_3 scale during accident scenarios with high-temperature steam. Alat et al. (2016) evaluated the performance of TiAlN/TiN multilayer coatings with different sublayers. Two multilayered coating designs with the largest number of sublayers (8- and 16-layered) showed the optimum protection against corrosion (i.e. minimum mass gain without spallation/delamination) at 360°C and 18.7 MPa up to 90 days. Figure 12 shows the corrosion rate and cross-sectional view as well as the corresponding EDS line scanning of TiAlN/TiN coatings after autoclave tests as an example. A thin layer of TiN (~1 µm) as a barrier on the surface was found to be sufficient to stop Al migration and prevent AlOOH phase formation during autoclave tests.

The coatings exhibited excellent corrosion resistance compared to uncoated Zircaloy; oxygen penetrated only to the outermost TiN layer with a depth of ~1.5 µm for the coatings with eight sublayers after 33 days of test (Figure 12B). Multilayer coatings with alternating sublayer architectures appear to be a promising solution for Zircaloy claddings to resist the extremely harsh environment in the nuclear core as well as to improve the accident tolerance. The performances of the coatings with respect to the in-core and accident conditions need to be proven for the sake of practical application.

3.6 Summarizing remarks

To evaluate Table 2 in a more straightforward approach, the performances of different types of coatings were assessed with regard to subcritical water corrosion and high-temperature steam oxidation. The performances have been categorized into five levels as shown in Figure 13 by interpreting their protective effect using bare Zircaloy cladding as benchmark. Additionally, it is assumed that coatings forming M_xO_y oxide scales during corrosion or oxidation are denoted as corresponding M-based coatings. In terms of coatings consisting of multiple elements or multilayers, such as FeCrAl, Ti_2AlC MAX phase, and TiAlN/TiN coatings, they are supposed to be of different base metals if distinctive oxide scales form during hot-water corrosion or steam oxidation.

The results suggest that Cr-based coatings perform excellent under both conditions due to the growth of a

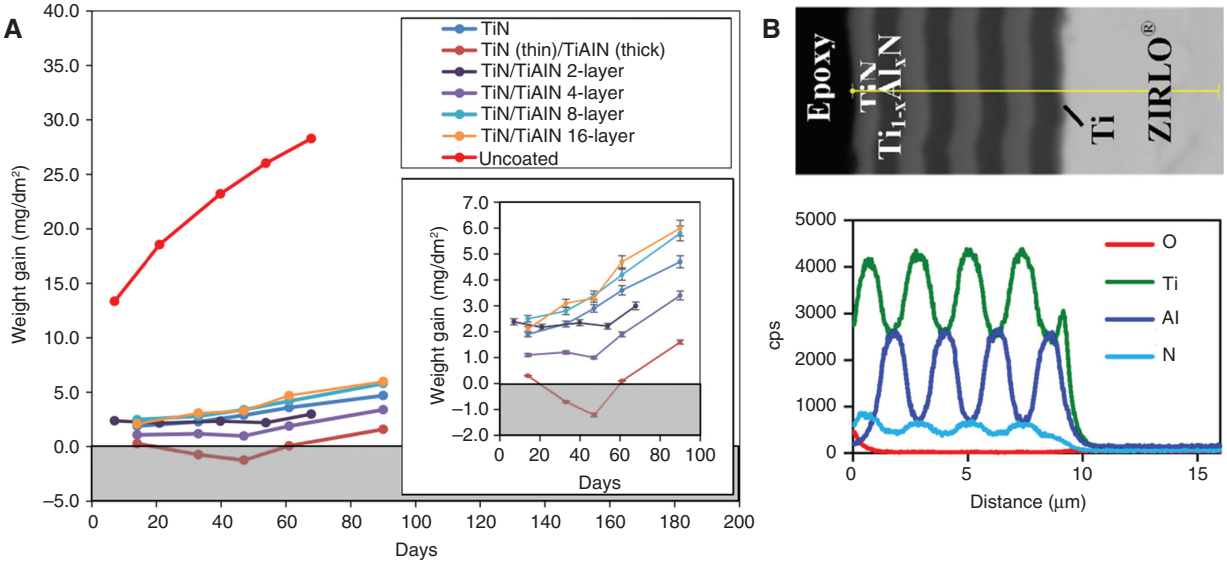

Figure 12: (A) Weight gain as a function of exposure time for TiN/TiAlN-coated samples with different sublayers tested in autoclave at 360°C and 18.7 MPa and (B) cross-sectional view and corresponding EDS line scanning of the coatings with eight sublayers after autoclave test for 33 days.
A thin surface oxide layer was observed. Reproduced from Alat et al. (2016) with permission from Elsevier.

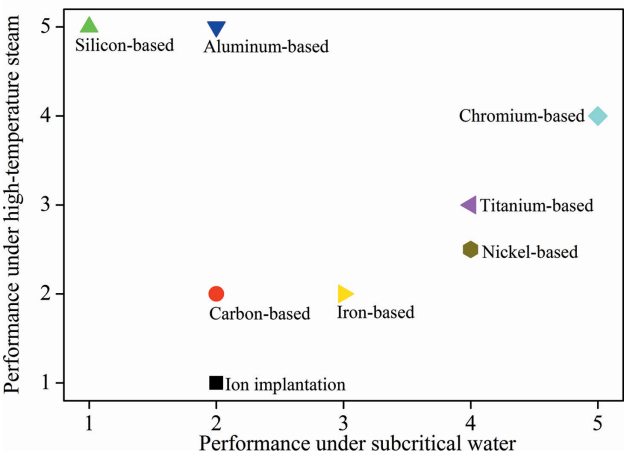

Figure 13: Authors' assessment of the performance of different types of coatings on Zr-based alloy claddings as ATF under normal and accident conditions; assuming M-based coatings form corresponding M_xO_y oxide scale during corrosion or oxidation (1, worst; …; 5, best).

protective Cr_2O_3 scale. The Cr_2O_3 scale acts as an efficient oxidant diffusion barrier during corrosion tests with one magnitude lower weight gain rate; hence, it is marked as highest grade 5 during hot-water corrosion. However, one limitation is that a Cr_2O_3 scale can only withstand temperatures up to ~1200°C when exposed to steam (marked as grade 4 during steam oxidation). The Al_2O_3 and SiO_2 scales, which provide excellent oxidation resistance for bulk materials at higher temperature in steam (grade 5, tolerance temperature higher than 1200°C), are found to be unstable during subcritical water corrosion (grades 1 and 2, no or little protective effect). However, it is necessary to mention that, in contrast to the bulk materials, all the Si- and Al-based coatings reported thus far failed to form dense SiO_2 or Al_2O_3 scales during high-temperature steam oxidation. Ti- and Ni-based coatings, followed by Fe-based coatings, show good performance under normal conditions, but their improvement under accident conditions (i.e. high-temperature steam) is limited as shown in Figure 13. Due to the formation of carbon oxide gases during corrosion and oxidation, carbon-based coatings are expected to improve somehow the performance only at low temperatures (grade 2).

4 Challenges of using coatings on Zr-based alloy claddings as ATF

The vast majority of approaches to improve the accident tolerance of current Zr alloy claddings reported in the past decades are based on the utilization of coatings and, to less extent, on using surface modification techniques. In terms of surface modifications, it seems that they are less suitable for ATF application, as the treated samples generally show better corrosion resistance but no or little improvement of high-temperature oxidation resistance in steam.

Generally, protective coatings that are developed to prevent underneath base materials from severe oxidation and corrosion at high temperature rely on the formation of a protective oxide scale on the surface. In an ideal situation, the oxide layer should be dense, slowly growing, highly stable, as well as adherent and coherent (Young, 2008). The most common and effective protective coatings are based on Cr_2O_3, Al_2O_3, and SiO_2 forming scales (Saunders et al., 2008). To at least maintain (if not improve) the fuel performance under normal operations while enhance the accident resistance and risk compatibility, some reasonably foreseeable requirements for surface modification (mainly utilization of coatings) of current Zr-based alloy claddings are urgently desired. The major requirements and challenges for protective coating-Zr-based alloy systems include the following:

- Capability to coat or treat full-length cladding tube with desired microstructure and acceptable cost;
- Relatively low fabrication temperature to avoid changing the microstructure of underlying Zr-based alloy;
- No or little negative effect on neutron economics;
- Good thermal properties (such as thermal conductivity and stability, comparable thermal expansion coefficients, and melting temperature);
- Good corrosion and irradiation resistance under normal operations that can survive for several fuel cycles;
- Good mechanical properties involving wear, fracture, spallation, and fretting-corrosion resistance under normal and accident conditions;
- Good adherence and ductility to sustain high viscoplastic deformation of Zr-based cladding in case of clad ballooning during accidental conditions; and
- Improved resistance to high-temperature steam or air under accident conditions.

4.1 Coating materials

Regarding the coatings reviewed, the coating materials can be divided into two major types: metallic coatings and ceramic coatings. Tables 3 and 4 conclude some noteworthy properties of various elements acting as coating components and their corresponding oxides reported previously (Matweb), respectively.

Table 4: Summary of the various properties for oxides.

Oxides	Density (g/cm^3)	Melting point (°C)	Thermal expansion ($\times 10^{-6}\ K^{-1}$, RT)	Thermal conductivity W/(m K), RT
ZrO_2	5.68	2715	12.0	1.67
SiO_2 (amorphous)	2.20	1715	0.54	1.46
Al_2O_3	3.96	2044	8.1	18.0–30.0
TiO_2 (rutile)	4.23	1855	7.14	7.40
Cr_2O_3	5.22	2435	7.1	10.0–32.9
Fe_2O_3	5.24	1565	~9.2	~15.0
NiO	6.67	1955	8.57	~20.2
Nb_2O_5	4.60	1512	~5.9	–
Y_2O_3	5.01	2425	~8.1	8–12

Metallic materials are the most common and important coating materials to protect a metallic system at elevated temperature with benefits of high ductility, good adherence due to the formation of a metallurgical bond with the substrate, high thermal conductivity (Table 3), and easy fabrication. However, some challenges often exist during practical service for metallic coatings. One disadvantage is the potential formation of brittle intermetallic compounds between the coating and the substrate during fabrication processes that can cause premature mechanical failure of the coating-substrate system. In addition, the high mutual diffusion rates, the mismatch of the thermal expansion coefficient (Table 3), and the formation of eutectic compounds at relatively low temperature between the coating and the substrate can promote in-service failure of the coatings or even aggravate the performance of the underneath substrate. These issues can potentially be avoided or mitigated through the adoption of an appropriate diffusion barrier (Park et al., 2016).

The ceramic coatings investigated are mainly carbides and nitrides with a small number of studies applying oxide coatings. One undesirable characteristic for oxide coatings is their low thermal conductivity (Table 4). This can influence the thermal flux in the core, increasing the temperature inside the cladding and making the core more susceptible to degradation. The low thermal conductivity of oxide coatings makes them less suitable for practical usage. Carbides and nitrides are more promising coating materials due to their excellent thermal and mechanical properties at elevated temperature as well as their high resistance to radiation damage. Besides, these coatings usually exhibit high hardness and good wear resistance, which supposes to improve the fretting-wear and fretting-corrosion resistance of the claddings against the coolant flow. One of the main challenges that need to be assessed for the adoption of ceramic materials as coatings is their brittle characteristic and weak toughness, making them prone to crack after experiencing high stresses (Liu et al., 2016). Previous fretting tests of TiN coatings on Zircaloy-4 revealed that the main wear mechanism was brittle rupture within the coating before destroying it (Sung et al., 2001). The mechanical integrity of coatings, especially ceramic coatings, during in-core service as well as high-temperature clad ballooning in LOCA scenarios requires specific attention in future studies.

For application in the nuclear core, neutron-transparent (i.e. with low thermal neutron absorption cross-section) materials are obviously appreciable (Wu et al., 2015). As shown in Table 3, thermal neutron absorption cross-sections for all the elements that have been used as coating components are <3, except for Ti (5.6) and Ni (4.5). Previous studies have suggested that it is necessary to minimize the coating thickness below 30 μm to limit neutronic penalties (Younker & Fratoni, 2016). Hence, in terms of thick coatings, for example, deposited by spraying processes, the Ti and Ni elements seem to be not applicable due to a pronounced effect on neutron economy.

4.2 Deposition technologies

Various technologies have been adopted to deposit coatings on Zr alloys, and they can be categorized into three main approaches: PVD, CVD, and spraying. Posttreatment was used in some cases to achieve the desired microstructure and properties of the coatings. Some other processes, such as electroplating or plasma electrolytic oxidation, were also used by some research groups. However, there is no follow-on investigation concerning coatings deposited by these methods until now. Furthermore, the published data suggest that these two processes are less suitable for practical applications due to the undesirable loose coating structure (Hui et al., 2011). The development of

novel surface treatment techniques, such as laser flashing or electron beam remelting, to densify the coating offers the potential to use these processes.

The majority of the work on the manufacturing protective coatings for Zr-based alloy claddings has been conducted using PVD processes primarily by sputtering techniques and arc ion evaporation. The PVD processes represent widely used techniques to deposit different kinds of thin-film coatings that use physical reaction, such as sputtering or evaporation, to produce a vapor of the target, which is then deposited on the substrate that requires coatings. Dense films with extremely smooth surface, good mechanical properties, and high adherence can be produced. Because PVD is a nonequilibrium process, the deposition of novel metastable materials with desired properties that are not restricted by classical thermodynamic properties and diffusion kinetics is feasible. The major obstacles for the selection of this technique are their relatively high cost due to the complex facility required and relatively low coating rates. The deposition rates are usually located in the range of below one to few microns per hour. The microstructure, composition, and performance of such coatings can be significantly influenced by the substrate surface conditions and process parameters. Several research groups have developed various generations of coatings by adjusting the process parameters to optimize the coatings (Alat et al., 2015; Brachet et al., 2015). In addition, the syntheses of some coatings require quite high substrate temperature or post-thermal treatment at relatively high temperature to obtain the desired microstructure, for example, Ti_2AlC MAX phase coatings at ~800°C (Tang et al., 2017) and Al coatings at 760°C (Carr et al., 2016). It is suggested that the process temperature is preferably below the final stress-relieved annealing (SRA) temperature (~450°C) of as-received Zr-based alloy claddings to avoid the modification of its mechanical and chemical properties. For coatings using PVD processes, the emphases are recommended to place on minimizing the processing times and temperatures as well as improving the reproducibility and reliability of the coatings.

Contrary to PVD, CVD processes are based on chemical reactions. In terms of depositing protective coatings on Zr alloys, it has only seen limited application for growing carbon-based coatings, such as PCD and SiC. The CVD processes usually run at much higher temperatures than PVD. Some researchers have shown that the substrate temperature can be reduced to quite a low level; however, the deposition rates simultaneously decrease. For instance, the growth rate for PCD film obtained at 450°C is below 20 nm/h (Ashcheulov et al., 2015), which will severely restrict the practical application of this process.

Another promising coating technique is spraying, such as cold spraying, laser spraying, and the HVOF process. The main advantages regarding such processes are their high deposition rates, low cost, and easy quality control. The major issues confronting the coatings deposited by this technique are that the coatings usually show a rough surface with relatively loose structure (Park et al., 2016). Besides, composition changes between the raw materials and the coatings are sometimes observed. Further investigations, such as by adjusting the process parameters or using posttreatment processes, are required to overcome these problems.

Each deposition process reviewed herein possesses its own benefits and limitations. The development of reliable and reproducible deposition processes, particularly PVD and spraying processes, with optimized coating performance and cost reduction is the primary recommendation for future R&D activities on coating manufacturing technology.

4.3 Stability under normal and accident conditions

The primary reason for the utilization of coatings on current Zr-based alloy claddings is to eventually improve the tolerance under transient accident conditions. Therefore, one prerequisite to achieve this goal is that the coatings must withstand the simultaneous occurrence of aqueous corrosion by hot water, irradiation damage, and various stresses during normal operations for a certain period of time, typically two to three fuel cycles. The high-temperature, high-pressure subcritical water used as coolant in the core is a highly reactive agent. Previous studies have demonstrated that typical structural metallic or nonoxide ceramic materials are converted into their oxides or dissolved rapidly by hydrothermal corrosion in hot water (Kritzer et al., 1999). Some materials hold good hydrothermal corrosion resistances that are attributed to the formation of a dense, adherent surface oxide layer that grows very slowly during long time exposure.

Pourbaix diagrams (i.e. electrochemical potential versus pH diagram for a given pressure, temperature, and dissolved ion concentration) are effective tools to evaluate the performance of a particular material, mostly metals, under the electrochemical corrosion in aqueous solutions. The diagrams can be classified into three regions of immunity, passivity, and corrosion related to the identities of the dominating species with respect to unreacted metal,

stable surface oxide, and aqueous ions, respectively (Cook & Olive, 2012a). Figure 14 shows the Pourbaix diagrams of six promising and widely used elements (Si, Al, Ti, Cr, Fe, and Ni) as coating components at 350°C, 25 MPa and ion concentration of 10^{-6} mol/kg (Allendorf et al., 1995; Cook & Olive, 2012a–c). Although the pressure here is a little higher than the typical PWR conditions, they can also provide some useful guidelines for the selection and development of the coating materials. The electrochemical potential and pH for the aqueous solution in PWR core are −500 mV_{SHE} and 7.0, respectively (Allen et al., 2012). Consistent with the previous autoclave corrosion results of various types of coatings, SiO_2- and Al_2O_3-forming materials are supposed to undergo severe attack with no protective effect due to the formation of soluble aqueous ions (Figure 14A and B). Metallic Ti, Cr, and Ni or corresponding-based materials are expected to exhibit passivity over a wide range of electrochemical potential and pH due to the

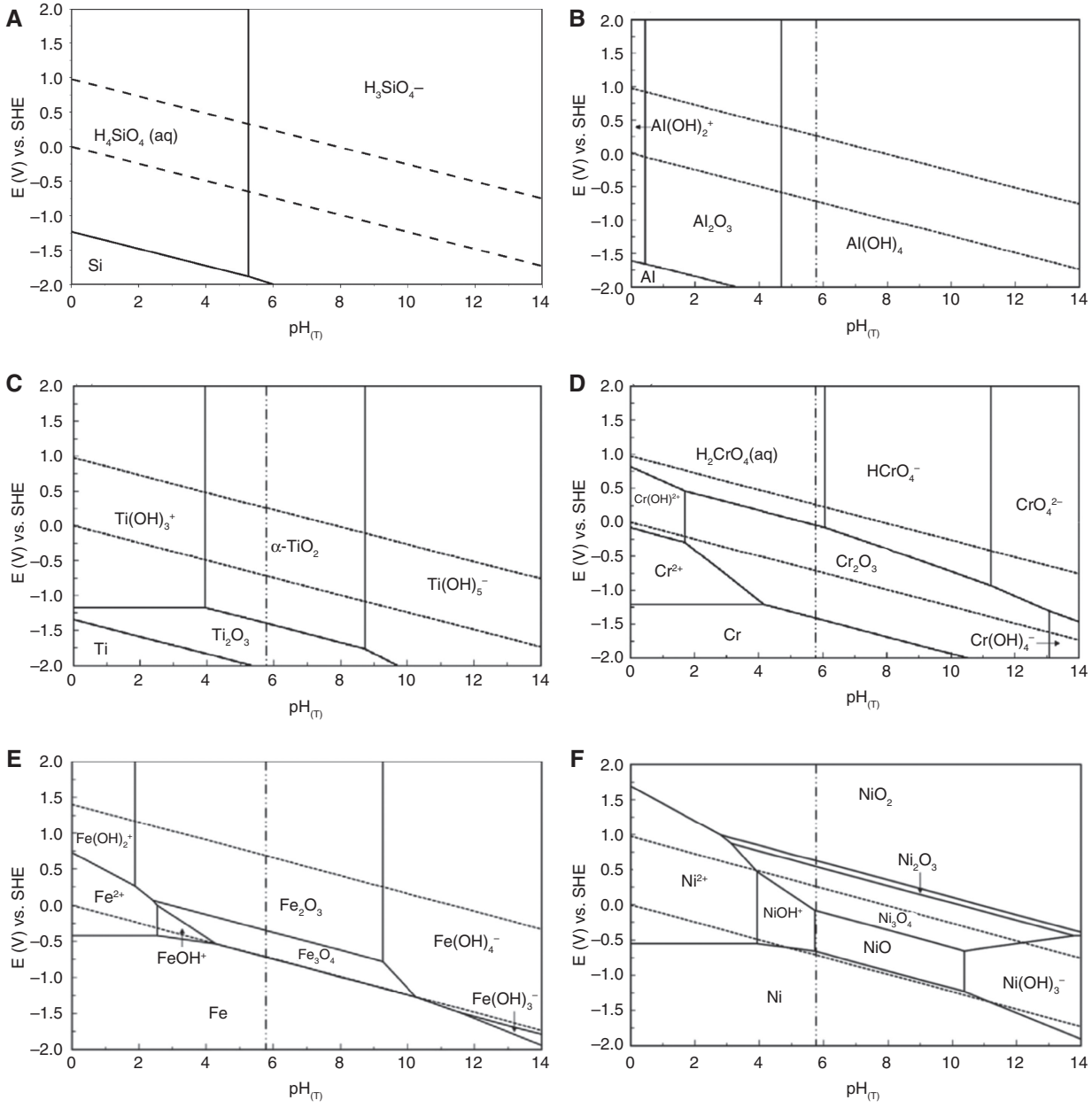

Figure 14: Pourbaix diagrams for (A) Si (calculated using HSC Chemistry software; Allendorf et al., 1995), (B) Al, (C) Ti, (D) Cr (Cook & Olive, 2012a), (E) Fe (Cook & Olive, 2012c), and (F) Ni (Cook & Olive, 2012b) at 350°C, 25 MPa and 10^{-6} mol/kg. SHE means standard hydrogen electrode.
Reproduced with permission from Elsevier.

formation of stable oxides (Figure 14C, D, and F). The stability or dissolution behavior of Fe-based materials is more complex and demonstrates susceptible to the water chemistry. According to Figure 14E, Fe oxides should be stable during normal operations. However, the dissolution of the Fe-rich spinel crystals resulted in net mass loss of some Fe-based alloys during autoclave test in simulated LWR water conditions (Terrani et al., 2016). Several passivity and corrosion regions are surrounded by each other near the PWR water conditions with decreasing pressure and ion concentration (Cook & Olive, 2012c). In summary, Cr, Ti, and Ni-based materials represent the optimum choices of coatings to resist the hydrothermal corrosion under normal conditions. It is necessary to mention that the majority of previous autoclave corrosion tests were performed in a static environment in which the dissolved aqueous ions can rapidly reach saturation. However, in a real situation, the coolant water flows at a rate of ~3600 kg/m^2 s (Cheng et al., 1996). Reducing the concentration of corrosion products typically results in increasing the size of corrosion areas while decreasing the passivity regions, for instance, Cr oxides are predicted to be unstable when the ion concentration reach 10^{-8} mol/kg at the same conditions (Cook & Olive, 2012a). Hence, the dissolution of the protective oxide layer in the core followed by precipitation at lower temperature regions leads to the potential causes of fast coating dissolution and breakdown. The stability of the protective oxide layers and the dissolution rates of corrosion products inside a core need to be fully investigated and fundamentally understood.

The initial evaluation of coating concepts on Zr-based alloys has focused on testing and verifying their feasibility under an out-of-pile situation. Another significant potential degradation phenomenon during in-pile service for the coatings is radiation damage and irradiation-assisted phenomena, such as phase transformation, irradiation hardening and growth, and interaction at the interface between the coated layer and the Zr-based alloy substrate. The irradiation performance of the coatings needs to be evaluated and the coatings must provide adequate resistance to irradiation that can maintain the protective effect during long time service. In addition, high magnitude stress can be accumulated within the coating-substrate system due to various factors, such as corrosion and irradiation-induced stress as well as mechanical stress like pellect-cladding-mechanical interactions (PCMI) upon power ramps. In an ideal situation, the coatings should be highly adherent during operation without spallation or cracking or can self-heal after the appearance of some defects. Additionally, it is important to demonstrate that various defects or partial spallation do not have a significantly negative impact on the benefits of the coating or the performance of the underlying fuel rod claddings. Above all, the comprehensive validation of the performance of the coated-Zr alloy cladding inside an in-pile operating environment for long time service remains an initial key step to provide practical acceptance.

Similar to hydrothermal corrosion, materials that provide good high-temperature steam and/or air oxidation resistance also depend on the formation of a dense and slow-growing oxide scale on the surface. The principal oxides that constitute the scale are mainly Cr_2O_3, α-Al_2O_3, and SiO_2. Generally, Cr_2O_3 scales have been proven to provide sufficient protection up to a maximum of ~1100°C–1200°C, α-Al_2O_3 to ~1400°C, and SiO_2 to ~1700°C in a long-term isothermal oxidation situation (Young, 2008). One notable feature of Cr_2O_3- and SiO_2-forming materials is that they may undergo active oxidation by forming volatile oxidation products rather than protective oxide scale especially in high-temperature steam depending on the local environment (Saunders et al., 2008; Terrani et al., 2014a). Nevertheless, α-Al_2O_3 and SiO_2 are the only two oxides that are capable of forming a very effective barrier against oxidation by steam up to extremely high temperature. However, these two oxides have been proven to be unstable under normal operations (Figure 14). A composite or multilayer coating concept with the capability of generating the corresponding stable and protective barrier under normal (hydrothermal corrosion) conditions and accident (steam oxidation) scenarios, respectively, which provides additional performance benefits, may be the appropriate coating choice. Generally speaking, the coating life is remarkably restricted by various issues at elevated temperature. A thorough survey is needed to be fulfilled to fundamentally understand the degradation mechanisms of the coated-Zr alloy claddings in simulated accident scenarios. Furthermore, it is necessary to prove that various defects within the coatings, rapture, or ballooning of the cladding that cause exposure of the inner fresh surface as well as loss of the protective effect of the coatings (for instance, due to oxidation, volatilization, interdiffusion, and chemical interactions with underneath substrate) will not cause faster oxidation or more rapid degradation of the then unprotected Zr alloy cladding substrate compared to the uncoated one during accident scenarios.

5 Conclusions

Various types of coatings have been proposed and examined to improve the performance of current Zr-based

alloy claddings, mainly regarding water side corrosion and high-temperature steam oxidation resistance, during normal and accident conditions. Cr-based coatings perform well under both conditions because of the successful growth of a protective Cr_2O_3 scale. The major obstacle is that Cr_2O_3 scale can only withstand the service temperature up to ~1200°C when exposed to steam. Al_2O_3 and SiO_2 scales, which can withstand higher temperatures in steam, are found to be unstable during subcritical water corrosion. Moreover, contrary to the behavior of bulk materials, all the Si- and Al-based coatings reported so far failed forming dense SiO_2 or Al_2O_3 scales during high-temperature oxidation. Ti- and Ni-based coatings, followed by Fe-based coatings, show good performance under normal conditions, but their improvement under accident conditions (i.e. high-temperature steam) are limited.

The performances of coatings are highly influenced by the composition and structure of the coating-substrate system, which rely on the deposition process and parameters. A detailed study for the selection of suitable fabrication process and deposition parameters should be conducted. The thickness for the application of coatings on the surface of Zr alloy claddings is restricted to not significantly change the behavior of the currently well-established Zr alloy clad/UO_2 fuel design. Therefore, thin, dense, and adherent coatings are favorable. As reviewed, most coating concepts simply concentrate on one special issue or scenario, and the comprehensive performance of the coating-substrate system under in-core situations is not yet developed. Considering the extremely harsh environment in nuclear core and high demands for improving safety and efficiency of current water-cooled reactors, single-layer coatings seem to be difficult to satisfy all these requirements. The major challenges for single-layer metallic or ceramic coatings are interactions between the coating and the substrate, such as fast interdiffusion rates and eutectic melt formation, at high temperature and their brittle characteristic, respectively. A composite coating system, such as composition gradient coating and functional gradient coating, providing extra performance benefits, may be the appropriate coating system for Zr-based claddings, which is fully qualified under various conditions. However, a complicated coating system certainly requires strict process control and quality control, which will also retard the licensing process under current regulatory criteria.

Acknowledgments: This work was supported by the Helmholtz (HGF) programs NUSAFE and STN at the KIT. It was further partially carried out with the support of the Karlsruhe Nano Micro Facility (KNMF; http://www.knmf.kit.edu). C. Tang acknowledges the China Scholarship Council (CSC No. 201406080013) for the PhD scholarship.

References

Abdelrazek ID, Sharkawy SW, El-Sayed HA. Pyrolytic carbon coating of Zircaloy-4 tubes at relatively low temperatures. J Nucl Mater 1997; 249: 159–164.

Al-Olayyan Y, Fuchs GE, Baney R, Tulenko J. The effect of Zircaloy-4 substrate surface condition on the adhesion strength and corrosion of SiC coatings. J Nucl Mater 2005; 346: 109–119.

Alat E, Motta AT, Comstock RJ, Partezana JM, Wolfe DE. Ceramic coating for corrosion (c3) resistance of nuclear fuel cladding. Surf Coat Technol 2015; 281: 133–143.

Alat E, Motta AT, Comstock RJ, Partezana JM, Wolfe DE. Multilayer (TiN, TiAlN) ceramic coatings for nuclear fuel cladding. J Nucl Mater 2016; 478: 236–244.

Allen TR, Konings RJM, Motta AT. Corrosion of zirconium alloys. In: Konings RJM, editor. Comprehensive nuclear materials. Oxford, UK: Elsevier, 2012: 49–68.

Allendorf MD, Melius CF, Ho P, Zachariah MR. Theoretical study of the thermochemistry of molecules in the Si-O-H system. J Phys Chem 1995; 99: 15285–15293.

Ashcheulov P, Škoda R, Škarohlíd J, Taylor A, Fekete L, Fendrych F, Vega R, Shao L, Kalvoda L,Vratislav S, Cháb V, Horáková K, Kůsová K, Klimša L, Kopeček J, Sajdl P, Macák J, Johnson S, Kratochvilova I. Thin polycrystalline diamond films protecting zirconium alloys surfaces: from technology to layer analysis and application in nuclear facilities. Appl Surf Sci 2015; 359: 621–628.

ASTM Standards. Standard guide for use of protective coating standards in nuclear power. ASTM Standards, West Conshohocken, PA, 2000: 1–8.

Azevedo CRF. Selection of fuel cladding material for nuclear fission reactors. Eng Fail Anal 2011; 18: 1943–1962.

Baney HR, Tulenko JS. An innovative ceramic corrosion protection system for Zircaloy cladding. No. DE-FG03-99SF21882. University of Florida, 2003.

Barsoum MW. The $M_{N+1}AX_N$ phases: a new class of solids; thermodynamically stable nanolaminates. Prog Solid State Chem 2000; 28: 201–281.

Brachet JC, Vandenberghe-Maillot V, Portier L, Gilbon D, Lesbros A, Waeckel N, Mardon JP. Hydrogen content, preoxidation, and cooling scenario effects on post-quench microstructure and mechanical properties of Zircaloy-4 and M5® alloys in LOCA conditions. In: Kammenzind B, Limbäck M, editors. Zirconium in the nuclear industry. 15th International Symposium, ASTM International, West Conshohocken, PA, 2009: 91–118.

Brachet JC, Saux M, Le Flem M, Le Urvoy S, Rouesne E, Guilbert T, Cobac C, Lahogue F, Rousselot J, Tupin M, Billaud P, Hossepied C, Schuster F, Lomello F, Billard A, Velisa G, Monsifrot E, Bischoff J, Ambard A. On-going studies at CEA on chromium coated zirconium based nuclear fuel claddings for enhanced accident tolerant LWRs fuel. In: Proceedings of 2015 LWR Fuel Performance/TopFuel, Zurich, Switzerland, September 13–19, 2015: 31–38.

Bragg-Sitton SM. Development of advanced accident-tolerant fuels for commercial LWRs. Nucl News 2014; 53: 83–91.

Carr J, Vasudevamurthy G, Snead L, Hinderliter B, Massey C. Investigations of aluminum-doped self-healing Zircaloy surfaces in context of accident-tolerant fuel cladding research. J Mater Eng Perform 2016; 25: 2347–2355.

Cathcart JV, Pawel RE, McKee RA, Druschel RE, Yurek GJ, Campbell JJ, Jury SH. Zirconium metal-water oxidation kinetics. IV. Reaction rate studies. ORNL/NUREG-17. Oak Ridge, Tennessee, USA: Oak Ridge National Laboratory, 1977.

Cheng B, Gilmore PM, Klepfer HH. PWR Zircaloy fuel cladding corrosion performance, mechanisms, and modeling. In: Bradley ER, Sabol GP, editors. Zirconium in the nuclear industry, 11th International Symposium, ASTM STP 1295, American Society for Testing and Materials, 1996: 137–160.

Chu S, Majumdar A. Opportunities and challenges for a sustainable energy future. Nature 2012; 488: 294–303.

Conrad JR, Radtke JL, Dodd RA, Worzala FJ, Tran NC. Plasma source ion-implantation technique for surface modification of materials. J Appl Phys 1987; 62: 4591–4596.

Cook WG, Olive RP. Pourbaix diagrams for chromium, aluminum and titanium extended to high-subcritical and low-supercritical conditions. Corros Sci 2012a; 58: 291–298.

Cook WG, Olive RP. Pourbaix diagrams for the iron-water system extended to high-subcritical and low-supercritical conditions. Corros Sci 2012b; 55: 326–331.

Cook WG, Olive RP. Pourbaix diagrams for the nickel-water system extended to high-subcritical and low-supercritical conditions. Corros Sci 2012c; 58: 284–290.

Gilbon D, Soniak A, Doriot S, Mardon JP. Irradiation creep and growth behavior, and microstructural evolution of advanced Zr-base alloys. In: Sabol GP, Moan GD, editors. Zirconium in the nuclear industry, 12th International Symposium, ASTM STP 1354, American Society for Testing and Materials, West Conshohocken, PA, 2000: 51–73.

Gu YF, Harada H, Ro Y. Chromium and chromium-based alloys: problems and possibilities for high-temperature service. J Metal 2004; 56: 28–33.

Hauffe K. Oxidation and corrosion of tin-coated Zircaloy-4. J Electrochem Soc 1976; 123: 595–602.

Hirano M, Yonomoto T, Ishigaki M, Watanabe N, Maruyama Y, Sibamoto Y, Sibamoto Y, Watanabe T, Moriyama K. Insights from review and analysis of the Fukushima Dai-ichi accident. J Nucl Sci Technol 2012; 49: 1–17.

Hui R, Cook W, Sun C, Xie Y, Yao P, Miles J, Olive R, Li J, Zheng W, Zhang L. Deposition, characterization and performance evaluation of ceramic coatings on metallic substrates for supercritical water-cooled reactors. Surf Coat Technol 2011; 205: 3512–3519.

Hwasung Y, Ben M, Robert M, David B, Xu P, Kumar S. Development of zirconium-silicide coatings for accident tolerant zirconium-alloy fuel cladding. In: Proceedings of International Congress on Advances in Nuclear Power Plants, ICAPP 2016, San Francisco, USA, April 17–20, 2016: 2126–2131.

Idarraga-Trujillo I, Flem MLE, Brachet JC, Saux MLE, Hamon D, Muller S, Vandenberghe V, Tupin M, Papin E, Monsifrot E, Billard A, Schuster S. Assessment at CEA of coated nuclear fuel cladding for LWRs with increased margins in LOCA and beyond LOCA conditions. In: Proceeding of LWR Fuel Performance Meeting/TopFuel, Charlotte, USA, September 15–19, 2013: 860–867.

International Atomic Energy Agency. IAEA Annual Report, 2014, 1–153.

Ivanova SV, Glagovsky EM, Nikonorov KY, Belugin II, Khazov IA. Methods to increase corrosion stability and wear resistance. In: Proceeding of LWR Fuel Performance Meeting/TopFuel, Charlotte, USA, September 15–19, 2013: 334–350.

Jeong YH, Park S, Lee M, Choi B, Baek J, Park J, LIM J, Kim H. Out-of-pile and in-pile performance of advanced zirconium alloys (HANA) for high burn-up fuel. J Nucl Sci Technol 2006; 43: 977–983.

Jin D, Yang F, Zou Z, Gu L, Zhao X, Guo F, Xiao P. A study of the zirconium alloy protection by Cr_3C_2-NiCr coating for nuclear reactor application. Surf Coat Technol 2016; 287: 55–60.

Khatkhatay F, Jiao L, Jian J, Zhang W, Jiao Z. Gan J, Zhang H, Zhang X, Wang H. Superior corrosion resistance properties of TiN-based coatings on Zircaloy tubes in supercritical water. J Nucl Mater 2014; 451: 346–351.

Kim HG, Kim IH, Jung YI, Park DJ, Park JY, Koo YH. High-temperature oxidation behavior of Cr-coated zirconium alloy. In: Proceeding of LWR Fuel Performance Meeting/TopFuel, Charlotte, USA, September 15–19, 2013: 842–846.

Kim HG, Kim IH, Jung YI, Park DJ, Park JY, Koo YH. Application of coating technology on zirconium-based alloy to decrease high-temperature oxidation. In: Comstock C, Barberis P, editors. Zirconium in the nuclear industry, 17th International Symposium, ASTM International, West Conshohocken, PA, 2014: 346–369.

Kim HG, Kim IH, Jung YI, Park DJ, Park JY, Koo YH. Adhesion property and high-temperature oxidation behavior of Cr-coated Zircaloy-4 cladding tube prepared by 3D laser coating. J Nucl Mater 2016; 465: 531–539.

Kritzer P, Boukis N, Dinjus E. Factors controlling corrosion in high-temperature aqueous solutions: a contribution to the dissociation and solubility data influencing corrosion processes. J Supercrit Fluids 1999; 15: 205–227.

Kuprin AS, Belous VA, Voyevodin VN, Bryk VV, Vasilenko RL, Ovcharenko VD, Tolmachova GN, Vygov PN. High-temperature air oxidation of E110 and Zr-1Nb alloys claddings with coatings. Probl Atmos Sci Technol 2014; 89: 126–132.

Kuprin AS, Belous VA, Voyevodin VN, Bryk VV, Vasilenko RL, Ovcharenko VD, Tolmachova GN, Vygov PN. Vacuum-arc chromium-based coatings for protection of zirconium alloys from the high-temperature oxidation in air. J Nucl Mater 2015; 465: 400–406.

Liu Y, Bhamji I, Withers PJ, Wolfe DE, Motta AT, Preuss M. Evaluation of the interfacial shear strength and residual stress of TiAlN coating on ZIRLO™ fuel cladding using a modified shear-lag model approach. J Nucl Mater 2016; 466: 718–727.

Luscher WG, Gilbert ER, Pitman SG, Love EF. Surface modification of Zircaloy-4 substrates with nickel zirconium intermetallics. J Nucl Mater 2013; 433: 514–522.

Maier BR, Garcia-Diaz BL, Hauch B, Olson LC, Sindelar RL, Sridharan K. Cold spray deposition of Ti_2AlC coatings for improved nuclear fuel cladding. J Nucl Mater 2015; 466: 712–717.

Matweb. Searchable database of material properties. Available at: http://www.matweb.com.

Mitsubishi. PWR Fuel, Mitsubishi Nuclear Fuel Co., Ltd. Available at: http://www.mnf.co.jp/en/business/product01.html.

Moalem M, Olander DR. Oxidation of Zircaloy by steam. J Nucl Mater 1991; 182: 170–94.

Motta AT, Couet A, Comstock RJ. Corrosion of zirconium alloys used for nuclear fuel cladding. Rev Mater Res 2015; 45: 311–343.
Nechaev A. Corrosion of zirconium alloys in nuclear power plants. IAEA, Vienna, IAEA-TECDOC-684, 1993: 1–177.
Nieuwenhove R, Van Daub K, Nordin H, Van Nieuwenhove R, Nordin H. Investigation of the impact of coatings on corrosion and hydrogen uptake of Zircaloy-4. J Nucl Mater 2015; 467: 260–270.
NRC. NRC Regulations Title 10, 50.46. Acceptance criteria for emergency core cooling systems for light-water nuclear power reactors.
Padture NP, Gell M, Jordan EH. Thermal barrier coatings for gas-turbine engine applications. Science 2002; 296: 280–284.
Pantano M, Avincola V, De Seze PA, McKrell T, Kazimi MS. High temperature steam oxidation performance of MAX phase (Ti_2AlC) coated ZIRLO. In: Proceedings of International Congress on Advances in Nuclear Power Plants, ICAPP 2014, Charlotte, USA, April 6–9, 2014: 2126–2135.
Park ST. Amorphous alumina oxidation protective coating for Zircaloy based on a compositional gradient layer system. Ph.D. thesis, University of Florida, 2004.
Park JH, Kim HG, Park J, Jung YI, Park DJ, Koo YH. High temperature steam-oxidation behavior of arc ion plated Cr coatings for accident tolerant fuel claddings. Surf Coat Technol 2015; 280: 256–259.
Park DJ, Kim HG, Jung Y, Park JH, Yang JH, Koo YH. Behavior of an improved Zr fuel cladding with oxidation resistant coating under loss-of-coolant accident conditions. J Nucl Mater 2016; 482: 75–82.
Peng DQ, Bai XD, Pan F, Sun H, Chen BS. Influence of aluminum ions implanted on oxidation behavior of ZIRLO alloy at 500°C. Vacuum 2006; 80: 530–536.
Pierson HO. Handbook of refractory carbides and nitrides: properties, characteristics, processing, and applications. Westwood, New Jersey, USA: Noyes Publications, 1996.
Roberts DA. Magnetron sputtering and corrosion of Ti-Al-C and Cr-Al-C coatings for Zr-alloy nuclear fuel cladding. Master's thesis, University of Tennessee, 2016.
Rogers KA. Fire in the hole: a review of national spent nuclear fuel disposal policy. Prog Nucl Energy 2009; 51: 281–289.
Sanz E, Vega C, Abascal JLF, MacDowell LG. Phase diagram of water from computer simulation. Phys Rev Lett 2004; 92: 255701.
Saunders SRJ, Monteiro M, Rizzo F. The oxidation behaviour of metals and alloys at high temperatures in atmospheres containing water vapour: a review. Prog Mater Sci 2008; 53: 775–837.
Schanz G, Adroguer B, Volchek A. Advanced treatment of Zircaloy cladding high-temperature oxidation in severe accident code calculations: part I. Experimental database and basic modeling. Nucl Eng Des 2004; 232: 75–84.
Skarohlíd J, Ashcheulov P, Jäger A, Racek J, Taylor A, Shao L. Nanosized polycrystalline diamond cladding for surface protection of zirconium nuclear fuel tubes. J Mater Process Technol 2014; 214: 2600–2605.
Sridharan K, Harrington SP, Johnson AK, Licht JR, Anderson MH, Allen TR. Oxidation of plasma surface modified zirconium alloy in pressurized high temperature water. Mater Des 2007; 28: 1177–1185.
Steinbrück M, Birchley J, Boldyrev AV, Goryachev AV, Grosse M, Haste TJ, Hózer Z, Kisselev AE, Nalivaev VI, Semishkin VP, Sepold L, Stuckert J, Vér N, Veshchunov MS. High-temperature oxidation and quench behaviour of Zircaloy-4 and E110 cladding alloys. Prog Nucl Energy 2010; 52: 19–36.
Steinbrück M, Vér N, Große M. Oxidation of advanced zirconium cladding alloys in steam at temperatures in the range of 600–1200°C. Oxid Met 2011; 76: 215–232.
Stueber M, Holleck H, Leiste H, Seemann K, Ulrich S, Ziebert C. Concepts for the design of advanced nanoscale PVD multilayer protective thin films. J Alloys Compd 2009; 483: 321–333.
Sung JH, Kim TH, Kim SS. Fretting damage of TiN coated Zircaloy-4 tube. Wear 2001; 250: 658–664.
Tallman DJ, Anasori B, Barsoum MW. A critical review of the oxidation of Ti_2AlC, Ti_3AlC_2 and Cr_2AlC in air. Mater Res Lett 2013; 1: 115–125.
Tang C, Stueber M, Steinbrueck M, Grosse M, Ulrich S, Seifert HJ. Assessment of high-temperature steam oxidation behavior of Zircaloy-4 with Ti_2AlC coating deposited by magnetron sputtering. In: Proceeding of the Nuclear Materials Conference, Montpellier, France, November 7–11, 2016.
Tang C, Klimenkov M, Jaentsch U, Leiste H, Rinke M, Ulrich S, Steinbrück M, Seifert HJ, Stueber M. Synthesis and characterization of Ti_2AlC coatings by magnetron sputtering from three elemental targets and ex-situ annealing. Surf Coat Technol 2017; 309: 445–455.
Terrani KA, Parish CM, Shin D, Pint BA. Protection of zirconium by alumina- and chromia-forming iron alloys under high-temperature steam exposure. J Nucl Mater 2013; 438: 64–71.
Terrani KA, Pint BA, Parish CM, Silva CM, Snead LL, Katoh Y. Silicon carbide oxidation in steam up to 2 MPa. J Am Ceram Soc 2014a; 97: 2331–2352.
Terrani KA, Zinkle SJ, Snead LL. Advanced oxidation-resistant iron-based alloys for LWR fuel cladding. J Nucl Mater 2014b; 448: 420–435.
Terrani KA, Pint BA, Kim YJ, Unocic KA, Yang Y, Silva CM, Silva CM, Meyer III HM, Rebak R. Uniform corrosion of FeCrAl alloys in LWR coolant environments. J Nucl Mater 2016; 479: 36–47.
Van Uffelen P, Konings RJM, Vitanza C, Tulenko J. Analysis of reactor fuel rod behavior. In: Cacuci DG, editor. Handbook of nuclear engineering. Boston, MA: Springer, 2010: 1519–1627.
Westwood ME, Webster JD, Day RJ, Hayes FH, Taylor R. Oxidation protection for carbon fibre composites. J Mater Sci 1996; 31: 1389–1397.
Wiklund U, Hedenqvist P, Hogmark S, Stridh B, Arbell M. Multilayer coatings as corrosion protection of Zircaloy. Surf Coat Technol 1996; 86: 530–534.
Wu X, Kozlowski T, Hales J. Neutronics and fuel performance evaluation of accident tolerant FeCrAl cladding under normal operation conditions. Ann Nucl Energy 2015; 85: 763–75.
Yeom H, Hauch B, Cao G, Garcia-Diaz B, Martinez-Rodriguez M, Colon-Mercado H, Olson L, Sridharan K. Laser surface annealing and characterization of Ti_2AlC plasma vapor deposition coating on zirconium-alloy substrate. Thin Solid Films 2016; 615: 202–209.
Young DJ. High temperature oxidation and corrosion of metals, 1st ed., Oxford, UK: Elsevier, 2008.
Younker I, Fratoni M. Neutronic evaluation of coating and cladding materials for accident tolerant fuels. Prog Nucl Energy 2016; 88: 10–18.
Zhong W, Mouche PA, Hana X, Heuser BJ, Mandapaka KK, Was GS. Performance of iron-chromium-aluminum alloy surface coatings

on Zircaloy 2 under high-temperature steam and normal BWR operating conditions. J Nucl Mater 2016; 470: 327–338.
Zinkle SJ, Was GS. Materials challenges in nuclear energy. Acta Mater 2013; 61:735–758.
Zinkle SJ, Terrani KA, Gehin JC, Ott LJ, Snead LL. Accident tolerant fuels for LWRs: a perspective. J Nucl Mater 2014; 448: 374–379.

Bionotes

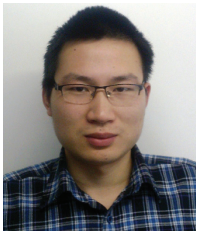

Chongchong Tang
Institute for Applied Materials (IAM),
Karlsruhe Institute of Technology (KIT),
D-76021 Karlsruhe, Germany

Chongchong Tang received his Master's degree in metallurgical engineering from the Northeastern University, China, in 2014. He is currently a PhD student in the IAM-AWP of the KIT in Germany. His research topic is the development of high-temperature oxidation-resistant coatings (MAX phase) for Zr-based alloy claddings and the investigation of the compatibility of candidate ATF bulk cladding materials (MAX phase and FeCrAl-RE alloys) in high-temperature steam.

Michael Stueber
Institute for Applied Materials (IAM),
Karlsruhe Institute of Technology (KIT),
D-76021 Karlsruhe, Germany

Michael Stueber is the group leader at the Department of Composites and Thin Films at the IAM of the KIT. He joined this team in 1992 and received his PhD in mechanical engineering from the University of Karlsruhe, Germany, in 1997. His R&D work since then is devoted to the development of high-performance thin films and coatings for engineering applications. His expertise is expressed in contributions on nearly 100 peer-reviewed scientific papers and several patents. His major contributions in recent years are on carbon-based composite coatings and novel oxide thin-film materials.

Hans Juergen Seifert
Institute for Applied Materials (IAM),
Karlsruhe Institute of Technology (KIT),
D-76021 Karlsruhe, Germany

Hans Juergen Seifert is the head of the IAM-AWP of the KIT and a professor in materials science and engineering. He received his PhD in materials science from the University of Stuttgart, Germany, in 1993. After working at the Max Planck Institute for Metals Research (Stuttgart, Germany), for Alstom (Birr, Switzerland), as an associate professor at the University of Florida (Gainesville, FL, USA), and as appointed professor by the Technical University of Freiberg (Germany), he joined the KIT in 2011. His main research areas are concerned with engineering materials for advanced energy technologies, including thermal and environmental barrier coatings, lithium batteries, gas turbines, and (nuclear) power plant technologies. He has published more than 160 peer-reviewed papers. He is the managing editor of the *International Journal of Materials Science* and the co-editor of two other journals.

Martin Steinbrueck
Institute for Applied Materials (IAM),
Karlsruhe Institute of Technology (KIT),
D-76021 Karlsruhe, Germany,
martin.steinbrueck@kit.edu

Martin Steinbrueck graduated with a degree in chemistry from the Friedrich Schiller University Jena and received his doctor of science in 1990. He has been with the KIT since 1991; in that time, he worked mainly in the field of nuclear safety research. Dr. Steinbrueck is the leader of the High-Temperature Materials Chemistry Group at the IAM. He is in charge of the KIT project QUENCH dealing with hydrogen source term and coolability during quenching of an overheated core in the framework of the KIT program on nuclear safety. His special interest is the materials behavior as well as the oxidation of and interactions between the various LWR core components at very high temperatures. He has published ~100 peer-reviewed papers.